INSTITUTO DE INGENIERÍA ENERGÉTICA
UNIVERSIDAD POLITÉCNICA DE VALENCIA

CPI, Edificio 8E, Cubo F, 5ª planta, Camino de Vera s/n, 46022 Valencia, Spain Tel. (34) 963877270, Fax (34) 963877272, Email: energeti@upvnet.upv.es

INSTITUTO DE INGENIERÍA ENERGÉTICA
(Institute for Energy Engineering)

Research Publications

Available online at www.sciencedirect.com

SciVerse ScienceDirect

journal homepage: www.elsevier.com/locate/ijrefrig

Numerical model for microchannel condensers and gas coolers: Part I – Model description and validation

Santiago Martínez-Ballester, José-M. Corberán, José Gonzálvez-Maciá*

Instituto de Ingeniería Energética, Universitat Politècnica de València, Camino de Vera s/n, Valencia 46022, Spain

ARTICLE INFO

Article history:
Received 30 January 2012
Received in revised form
26 August 2012
Accepted 27 August 2012
Available online 6 September 2012

Keywords:
Condenser
Model
Heat conduction
Microchannel
Fin
Gas cooler

ABSTRACT

The present work presents a model (Fin1Dx3) for air-to-refrigerant microchannel condensers and gas coolers, with any refrigerant circuitry. The model applies a segment-by-segment discretization to the heat exchanger, adding in each segment a novel bi-dimensional discretization to the fluids flow, fin and tube wall. Fin1Dx3 introduces a new approach to model the air-side heat transfer by using a composed function for the fin wall temperature, which allows to take into account more fundamentally the heat conduction between tubes. The proposed model accounts for: 2D longitudinal heat conduction in the tube wall, the heat conduction between tubes along the fin, and the unmixed air influence on performance. The paper presents the heat exchanger discretization, the governing equations, the numerical scheme employed to discretize equations and the solving methodology. The model has been validated against experimental data for both a condenser and a gas cooler, resulting in predicted capacity errors within ±5%.

Modèle numérique pour les condenseurs à microcanaux et les refroidisseurs de gaz : Partie I – Description et validation du modèle

Mots clés : Condenseur ; Modèle ; Conductivité thermique ; Microcanal ; Ailette ; Refroidisseur à gaz

1. Introduction

The use of microchannel heat exchangers (MCHXs) is increasing because of their compactness and high effectiveness. In the case of transcritical CO_2 systems, microchannels have an additional merit related to their high mechanical strength.

Nowadays, simulation software is a very suitable tool for the design of products in which complex physical processes occur. These tools allow us to save lots of costs and time in the laboratory working with expensive test benches. Currently, several models or simulation tools for heat exchangers are available in the literature: for finned tubes (CoilDesigner, 2010; Corberán et al., 2002; EVAP-COND, 2010; IMST-ART, 2010; Jiang

* *Corresponding author*. Tel.: +34 963 879 121; fax: +34 963 879 126.
E-mail address: sanmarba@iie.upv.es (S. Martínez-Ballester).
0140-7007/$ – see front matter © 2012 Elsevier Ltd and IIR. All rights reserved.
http://dx.doi.org/10.1016/j.ijrefrig.2012.08.023

Nomenclature

A	heat transfer area (m^2)
Ac	cross-sectional area (m^2)
Cp	specific heat ($J\ kg^{-1}\ K^{-1}$)
D	hydraulic diameter (m)
f	Darcy–Weisbach friction factor
g	gravitational constant ($m\ s^{-2}$)
H	height (m)
h	specific enthalpy ($J\ kg^{-1}$)
k	thermal conductivity ($W\ m^{-1}\ K^{-1}$)
l	distance between two wall cells (m)
LHC	longitudinal heat conduction
$\dot{m}$	mass flow rate ($kg\ s^{-1}$)
N	number of cells
N_s	number of segments
NTU	number of transfer units
P	wetted perimeter (m)
p	pressure (Pa)
$\dot{q}$	heat flux ($W\ m^{-2}$)
s	length in the forward direction of a fluid (m)
T	temperature (K)
t	thickness (m)
U	overall heat transfer coefficient ($W\ m^{-2}\ K^{-1}$)
V	volume (m^3)
X, Y, Z	spatial coordinates (m)

Greek symbols

α	convective heat transfer coefficient ($W\ m^{-2}\ K^{-1}$)
β	tube orientation (deg)
ε	heat exchanger effectiveness
φ	fin height ratio
θ	temperature difference (K)
ρ	density ($kg\ m^{-3}$)

Subscript

a	air, air cell index
acc	acceleration
cont	contraction
exp	expansion
f	fin, fin cell index
fB	fin cell at bottom
fr	friction
fT	fin cell at top
g	gravitational
i	fluid cell index
in	inlet
j	matrix column index
k	tube direction index
N, S, W, E, J_B, J_T	directions of neighbour wall cell
out	outlet
r	refrigerant, refrigerant, cell index
t	tube, tube cell index
X, Y, Z	spatial coordinates directions

et al., 2006; Lee and Domanski, 1997; Singh et al., 2008) and microchannel heat exchangers (Asinari, 2004; Fronk and Garimella, 2011; García-Cascales et al., 2010; Shao et al., 2009; Yin et al., 2001). Some of them (Asinari, 2004; CoilDesigner, 2010; Corberán et al., 2002; IMST-ART, 2010; Shao et al., 2009; Singh et al., 2008; Yin et al., 2001) apply energy conservation equations to each control volume, while others (Fronk and Garimella, 2011; García-Cascales et al., 2010; Jiang et al., 2006; Lee and Domanski, 1997; EVAP-COND, 2010) apply directly the solution given by the ε-NTU methodology. The main difference between the two methodologies is that the ε-NTU model has several implicit assumptions resulting in less freedom to describe the actual processes. Despite this fact, the models that do not apply the ε-NTU methodology usually make the same assumptions for the thermal problem as those used by ε-NTU based models, of which the most important for the aim of this paper are the following:

- Negligible effect of 2D longitudinal heat conduction (LHC).
- No heat conduction between tubes along the fin (adiabatic-fin-tip assumption).
- Application of the fin theory, which assumes uniform air temperature along the fin height.

Some of these assumptions have been studied in the literature for some heat exchanger topologies, such as finned tubes heat exchangers, whilst the effects of these assumptions are not studied so extensively for parallel tubes and serpentine MCHXs. These heat exchangers have a different thermal behaviour since the thermal and geometric conditions are different. Thus, it is interesting to evaluate the impact of the classical assumptions, which were explained previously, on the model results. Martínez-Ballester et al. (2011) performed a literature review in which the influence of all these effects was investigated theoretically and experimentally for both finned tubes and MCHXs.

The main motivation for this work is based on the drawbacks that, in the authors' opinion, existing models have when they are applied to some recent designs of heat exchanger, such as serpentine and parallel tubes MCHXs.

Firstly, Martínez-Ballester et al. (2011) proposed a model for a microchannel gas cooler referred to as the Fin2D model. The model subdivides the heat exchanger into segments, and these segments are divided into cells, to which the corresponding system of energy-conservation equations is applied without traditional heat exchanger modelling assumptions: the model accounts for 2D LHC in the tube and fin wall; it does not use any fin efficiency so it can model consistently the heat conduction between tubes. Since it applies a 2D discretization for the air in each segment, it does a more accurate integration of the heat transferred from the fin to the air, since the air temperature is more uniform in a cell. In contrast, most of the models apply the fin theory that assumes intrinsically uniform air temperature along the fin height. Furthermore, the Fin2D model allows independent discretization to be applied for refrigerant and air. This fact is interesting to capture the variation in air properties along the air flow direction.

The aim of developing the Fin2D model was to evaluate the prediction errors of the classical modelling assumptions and techniques described above, in an equivalent piece of

a microchannel gas cooler, and identify error sources. A microchannel gas cooler working with CO_2 in supercritical pressures was the application chosen because it is an application where a large impact on the performance can be expected due to 2D LHC in the tube wall and heat conduction between tubes along the fins. The reasons are based on the temperature glide of CO_2 during a supercritical gas cooling, in contrast with a condenser where the temperature during condensation is approximately constant. The conclusions of the studies by Martínez-Ballester et al. (2011), related to this work, were as follows:

- The impact of LHC effects along each direction in the fins and tube walls, if considered separately, was not significant. The combined effect was more noticeable and resulted in a capacity prediction error of as much as 2.5%, with the LHC in the tube, along the air flow direction, being the dominant effect. The impact of LHC depends on the air-side heat transfer coefficient.
- Use of the adiabatic-fin-tip efficiency, which is commonly applied, leads to large errors in heat distribution per tube when a temperature difference between tubes exists, i.e. when heat conduction between tubes exists. In addition, this assumption affects the global capacity prediction for microchannel gas coolers with a large number of refrigerant passes. Thus, the fin cuts are justified in these heat exchanger topologies.
- The temperature of air close to the tube wall is very different from the bulk air temperature. This fact could have an important impact on local effects controlling the heat and mass transfer, e.g. dehumidification. It would be interesting to evaluate the isolated effect of the non-uniform temperature profile of the air along the fin height.

The case studied by Martínez-Ballester et al. (2011) consisted of two tubes with a tube length of 8 cm and only one refrigerant pass. This case study was sufficient to identify the deficiency sources of the classical methodologies in this kind of heat exchanger, but was no good for evaluating the global performance prediction errors when an actual MCHX is simulated regarding dimensions, number of tubes and number of refrigerant passes. The main reason which prevented the study of an actual microchannel gas cooler was the computational cost of the Fin2D model. This model has a large computational cost, mainly due to the fin surface discretization: the model needs to employ a large number of fin cells because any fin efficiency is used to solve the heat transfer equation along the fin, which involves heat convection and heat conduction. Furthermore, the Fin2D model applies the same discretization for both air and fin, so the air also introduced an important computational effort.

One of the most important effects to capture, in the authors' opinion, is the heat conduction between tubes. Some authors Lee and Domanski (1997) and Singh et al. (2008) have implemented this heat conduction phenomenon in their corresponding models for finned tube heat exchangers. In order to implement it, they apply similar approaches, which will be discussed in Part II (Martínez-Ballester et al., submitted for publication), that consist in adding a heat conduction term to the energy conservation equation in the tube wall. The energy conservation equation in the tube wall includes the heat transfer from fin to air that is modelled by using fin efficiency. This fin efficiency is based on the fin theory, whose application was discussed above, assuming an adiabatic-fin-tip in order to evaluate the fin efficiency. Then, they introduce the heat conduction term as a function of the temperature gradient between neighbouring tubes. Singh et al. (2008) apply to this term a multiplier which has to be adjusted either numerically or experimentally. These multipliers are dependent on several factors, including the type of fin (slit, louvered, etc.) and ratio of row and tube pitch to tube outer diameters. However, Singh et al. (2008) concluded that more analysis needs to be done to analytically obtain these multipliers. Basically, this approach corrects a scenario where the adiabatic-fin-tip assumption is not satisfied by applying a correction term to take into account heat conduction between tubes. To this end, the authors developed the model presented in this paper with a proper formulation to take into account heat conduction between tubes without applying the adiabatic-fin-tip assumption, thus no correction term was needed.

Asinari (2004) developed one of the most accurate models for MCHX available in the literature. The model discretizes the fins along the air flow direction into a number of fin elements. Each fin element is modelled by means of the analytical 2D solution according to the classical theory for extended surfaces heat transfer. On the other hand, to apply this analytical solution Asinari (2004) has to assume a uniform air temperature over the whole the fin element, which means that the 1D solution becomes quite similar to the 2D solution. However, the authors found in Martínez-Ballester et al. (2011) that the effect of the temperature variation of the air temperature along the height of the fin has a considerable effect on the solution.

Summarizing all the motivation explained above, the goal of the present work is to develop a model based on the Fin2D model, without modelling the negligible effects and changing the model structure and/or discretization in order to reduce the computational cost, providing a simulation tool for MCHXs with reasonable computational cost for design purposes. The result is a much faster model with almost the same accuracy as the Fin2D model. Finally, given this computational time reduction, the proposed model is able to simulate either a microchannel gas cooler or a condenser with any refrigerant circuitry. Part II (Martínez-Ballester et al., submitted for publication) will employ the proposed model as a simulation tool to assess the impact of some design parameters of an MCHX. Some of these numerical studies are novel in the literature because they require a model which takes into account all the phenomena described above.

The present work has been aimed at developing a new model for microchannel heat exchangers which can take into account the heat transfer processes with more accuracy, paying attention also to the computational cost. The main differences of the proposed model with regard to the rest of current models in literature are: to be able to apply the fin theory in a more fundamental way, to take into account implicitly the heat conduction between tubes without using a fin efficiency and the novel numerical scheme developed to solve the problem with a good computational cost.

2. Model description

The model proposed in this paper, which will be referred to as Fin1Dx3, is based on the Fin2D model presented by Martínez-Ballester et al. (2011), performing some changes in order to reduce the computational cost but preserving accuracy. The changes are based on the following considerations:

- The study of Martínez-Ballester et al. (2011) revealed that the longitudinal conduction in the fin along the air flow direction resulted in a negligible effect on the predicted performance results. In addition, several current fin surfaces have cuts along this direction (louvered, slit, lanced…), which cancel LHC in that direction. Thus, in the present model this effect is cancelled, which means in practice no thermal connections between neighbouring fin cells along the air flow direction, even though a discretization of both the fin and air exists along this direction.
- The study of Martínez-Ballester et al. (2011) revealed that the air temperature profile is quite flat along the direction between tubes, excepting the air close to the tube wall. In that study the height of fin occupied by the air close to the tube with a temperature different from the rest of the air was about 1/30 of the total fin height. The discretization of air along that direction increases the computational cost. On the other hand, it would be quite interesting to capture the effect of accounting for the temperature difference between the air close to the tube wall and the rest of the air. A possible solution for this conflict of interests is to discretize the air with three air cells along the Y direction, as shown in Fig. 1. For this discretization, the height of the air cells close to the tube wall will be adjusted either experimentally or numerically. The only restriction is that both fin cells (cells close to the tubes), for the same Z, will measure the same. What these three air cells actually represent is the consideration of non-mixed air along the Y direction between them. This idea makes sense for air flowing through louvered fins and for laminar flows, i.e., the air could be assumed as mixed along all the louver height but as non-mixed with the rest of the air close to the tube walls, since the fin height is greater than the louver height, as shown in Fig. 1; laminar flow represents a non-uniform temperature distribution along the Y direction.

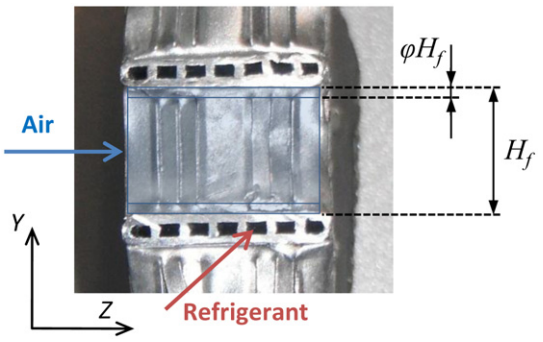

Fig. 1 – Detail of a louvered fin surface in a microchannel heat exchanger, where the non-louvered height and the total fin height are depicted.

- The Fin2D model solved the heat transferred from the air to the fin without applying the fin theory. Consequently, the Fin2D model needs a large number of fin cells along the Y direction in order to solve accurately the 2D heat conduction in the fin. This calculation is the procedure which required more computational cost within the Fin2D model.

The fin temperature, for a uniform fin, is governed by Eq. (1). Only when the air temperature is constant, Eq. (1) can be expressed as Eq. (2) (Incropera and DeWitt, 1996). If heat transfer properties are constant, or they are evaluated with mean values, the general solution for Eq. (2) is Eq. (3).

$$\frac{d^2T_f}{dY^2} - m^2(T_f - T_a) = 0 \tag{1}$$

$$\frac{d^2\theta_{f,a}}{dY^2} - m^2\theta_{f,a} = 0 \tag{2}$$

$$m^2 = \frac{\alpha\, P}{k\, A}$$

$$\theta_{f,a}(Y) = C_1 e^{mY} + C_2 e^{-mY} \tag{3}$$

Thus, the main assumption of the fin theory which is not satisfied in an actual fin surface is that the air temperature is not uniform along the Y direction. In the model proposed in this paper, the discretization for the fin and the air is the same and the discretization in the air has been chosen in order to represent air cells with uniform temperature, so it could be possible to apply the fin theory solution (Eq. (3)) for each air-fin cell connection without failing the assumption of uniform air temperature. The result of this methodology is a great reduction, in comparison with Fin2D, of the grid size and consequently of the computational cost.

It should be noted that Eq. (3) does not imply the classical adiabatic-fin-tip assumption (in the cross-section at half fin height), since boundary conditions have not been applied yet. The evaluation of the constants C_1 and C_2 will be explained in Subsection 2.2.3.

2.1. *Heat exchanger discretization*

Fig. 2 presents an example of an MCHX that can be simulated with the proposed model. The model can simulate any refrigerant circuitry arrangement: any number of refrigerant inlets and outlets; and any connection between different tube outlets/inlets at any location.

Fig. 3 shows the discretization in segments of the heat exchanger shown in Fig. 2, where the thinner lines correspond to thermal connections between wall cells, whereas the thicker lines correspond to the refrigerant flow path. First, the heat exchanger is discretized along the X direction (refrigerant flow), resulting in N_s segments per tube. The discretization for each segment is the same and is shown in Fig. 4. Each segment consists of: a refrigerant stream that is split into $N_{r,\,Z}$ channels in the Z direction; a flat tube which is discretized into $N_{t,\,Z}$ cells in the Z direction; and both air flow and fins, which are discretized in two dimensions: $N_{a,\,Y} = 3$ cells in the Y direction and $N_{a,\,Z}$ cells in the Z direction. Since the discretization for the air and fin wall is the same, $N_{f,\,Y} = N_{a,\,Y}$ and $N_{f,\,Z} = N_{a,\,Z}$.

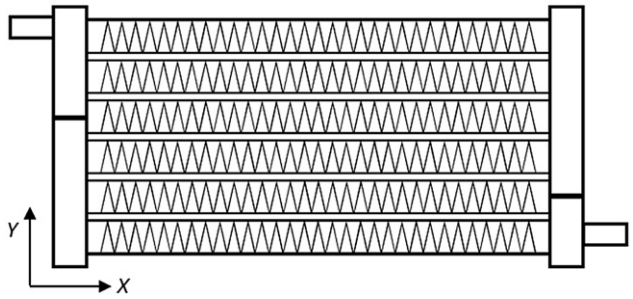

Fig. 2 – Example of a microchannel heat exchanger that can be simulated by Fin1Dx3.

The discretization for a heat exchanger is summarized in the following as a grid: {N_s, $N_{r,z}$, $N_{t,z}$, $N_{a,z}$}. For illustration of the nomenclature, the numerical example shown in Figs. 3 and 4 corresponds to a grid: {3,4,3,2}.

The refrigerant flows inside the channels along the *X* direction without any mixing between the channels, and it exchanges heat with the tube cells in contact; these tube cells transfer heat to the air cells in contact by convection, to their neighbouring tube cells on the plane *X*-*Z* by conduction, and to the fin roots in contact by conduction. The air exchanges heat by convection with the fin cells, and the air cells at the bottom and top also exchange heat with the tube cells in contact. The fin cells conduct the heat along the *Y* direction, and the bottom and top fin cells also conduct heat to the neighbouring tube wall.

Regarding the fluid cells, either air or refrigerant, there are two typologies: elemental cell and mixture cell. The elemental cell corresponds to the one described above, exchanging heat with the surrounding wall cells. The mixture cell is adiabatic and its function is collecting the fluid from a number of tubes and distributing it into the next tubes according to the heat exchanger circuitry. The inlet and outlet ports of each tube are connected to the corresponding mixture cells. The distribution of these fluid cells and the definition of the tubes connected to these cells determine the flow path of each fluid. In the proposed model, any configuration can be fixed, thus heat exchangers such as serpentine or parallel tube MCHXs can be simulated with any refrigerant circuitry.

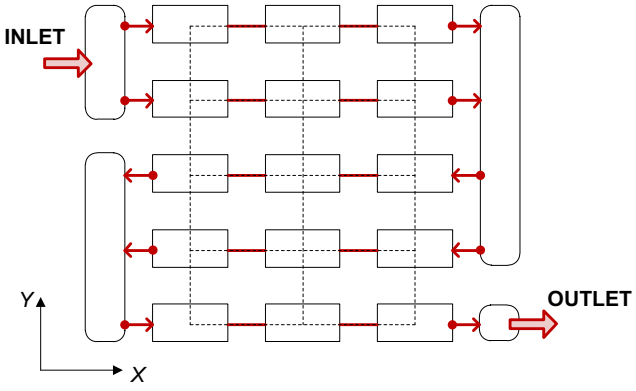

Fig. 3 – Discretization in segments of the heat exchanger shown in Fig. 2, which includes the thermal connections between different segments and flow arrangement.

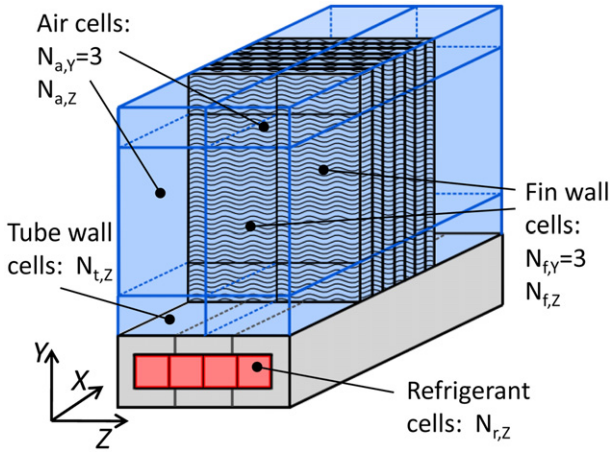

Fig. 4 – Schematic of a segment discretization into cells.

The model is designed to allow this methodology also with air, but in this work, these mixture cells were only used for the refrigerant fluid. In Fig. 3, these refrigerant cells are represented by the round shape boxes.

2.2. *Governing equations*

Every fluid cell (either refrigerant or air) has two nodes, which correspond to the inlet and outlet sections in the fluid flow direction. The tube wall cells have only one node located in the centroid of the cell, as shown in Fig. 5(a). All cell local variables are referred to the value in these nodes, e.g. $T_{r,\,in}$ and $T_{r,\,out}$ are the temperature at the inlet and outlet, respectively, of a refrigerant cell *r*; for the air flow these would be the same but with subscript *a*; T_t is the temperature of the tube cell *t*. The fin does not have any node because a continuous function governs in the fin.

According to the assumptions and methodology explained above, the governing equations for the tube wall will be different from those applied to the fin wall. So, the description of the governing equations is going to be structured in four blocks: refrigerant flow, air flow, tube wall and fin wall, with their corresponding thermal connections between neighbouring fluids or wall cells.

2.2.1. *Tube wall and its thermal connections*

The energy conservation equation for a tube cell can be written as:

$$\nabla(k_{t,k}\nabla T_t)\mathrm{d}V + \sum_{r=1}^{n_r} \dot{q}_{t,r} P_{t,r}\mathrm{d}s_{t,r} + \sum_{a=1}^{n_a} \dot{q}_{t,a} P_{t,a}\mathrm{d}s_{t,a} = 0 \qquad (4)$$

where any tube wall cell *t* is in contact with n_r refrigerant cells $r = 1, n_r$ and with n_a air cells $a = 1, n_a$; $k_{t,k}$ is the thermal conductivity of the tube cell *t* in the *k* direction. The Laplacian term is the term that allows us to study the influence of 2D LHC along the tube walls, and it also takes into account the heat transferred by conduction between a tube cell and the adjoined fin cells. The heat fluxes $\dot{q}_{t,r}$ and $\dot{q}_{t,a}$ for a thermal connection between a tube wall cell *t* and a fluid cell *i*, either air or refrigerant, are evaluated as follows:

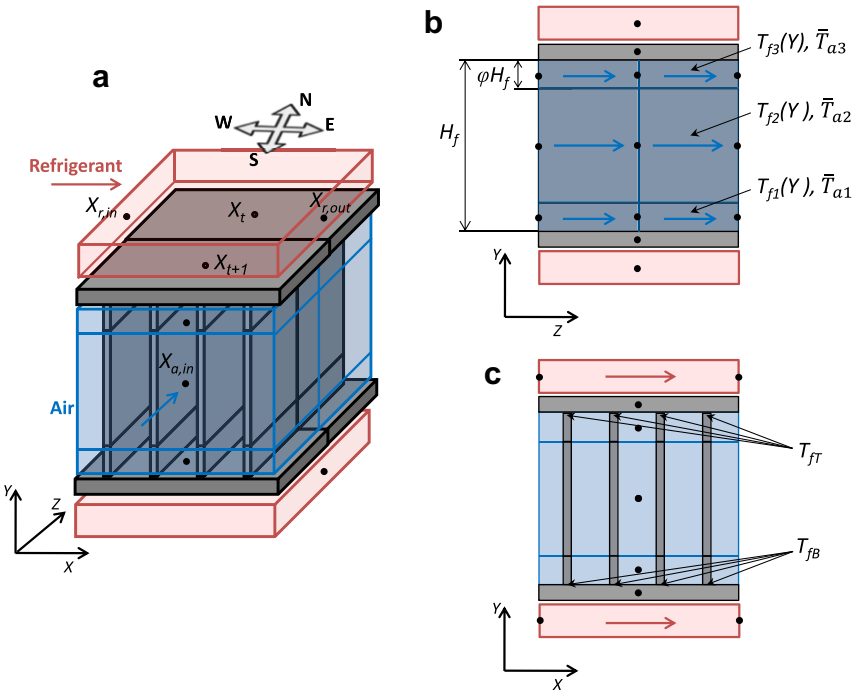

Fig. 5 – Different views of a discretized portion of the heat exchanger: (a) global view illustrating fluid nodes and tube directions; (b) Z-Y plane, which shows main geometric data of the fin and regions in which is defined the corresponding $T_f(Y)$ and $\bar{T}_a$; (c) X-Y plane, which shows the location of the T_{fT} and T_{fB} temperatures.

$$\dot{q}_{t,i} = U_{t,i}(T_t - T_i) \tag{5}$$

where the overall heat transfer coefficient $U_{t,i}$ for this connection corresponds to:

$$U_{t,i} = \frac{1/A_{t,i}}{\frac{t_t/2}{A_{t,i}k_{t,k}} + \frac{1}{A_{t,i}\alpha_{t,i}}}$$

The different correlations employed to evaluate the heat transfer are listed in Table 1. By using Eq. (5), Eq. (4) can be rewritten as follows:

$$\nabla(k_{t,k}\nabla T_t)dV + \sum_{i=1}^{n_i} P_{t,i}U_{t,i}\,(T_t - T_i)\,ds_{t,i} = 0 \tag{6}$$

where $n_i = n_r + n_a$.

2.2.2. *Refrigerant flow*

Eq. (7) states the energy conservation for a refrigerant cell r in contact with n_t tube wall cells $t = 1, n_t$.

$$\dot{m}_r dh_r = \sum_{t=1}^{n_t} \dot{q}_{t,r} P_{t,r} dX \tag{7}$$

The fluid pressure drop along the length of the refrigerant cell, r, is obtained by integration of the momentum equation:

$$\Delta p_r = \Delta p_{r,fr} + \Delta p_{r,acc} + \Delta p_{r,g} \tag{8}$$

where the friction term is evaluated in the form:

$$\Delta p_{r,fr} = f_r \frac{\Delta X_r}{D_r A c_r^2 (\rho_{r,in} + \rho_{r,out})} \dot{m}_r^2 \tag{9}$$

The friction factor f_r can be evaluated by several correlations available in the literature. The correlations employed to evaluate the pressure drop coefficients are listed in Table 1. The void fraction was modelled as separated-flow, adopting Chisholm's (1972) correlation for the slip ratio. The acceleration term can be expressed by:

$$\Delta p_{r,acc} = \left(\frac{\dot{m}_r}{Ac_r}\right)^2 \left(\frac{1}{\rho_{r,out}} - \frac{1}{\rho_{r,in}}\right) \tag{10}$$

Table 1 – Correlations used in the model for coefficients evaluation.

	Heat transfer coefficient	Pressure drop	Expansion/Contraction pressure losses
Refrigerant			
One-phase	Gnielinski (1976)	Churchill (1977)	Kays and London (1984)
Two-phase	Cavallini et al. (2002)	Friedel (1980)	Kays and London (1984)
Air			
	Kim and Bullard (2002)	Kim and Bullard (2002)	Kays and London (1984)

Finally, the gravitational term can be evaluated as follows:

$$\Delta p_{r,fr} = \frac{1}{2} g(\rho_{r,\text{in}} + \rho_{r,\text{out}}) \Delta X_r \sin\beta \tag{11}$$

The mixture cells, which in this work are only used for the refrigerant flow, have another formulation since they are adiabatic and only collect and/or distribute the refrigerant flow. The governing equations implemented in these cells determine whether the fluid flow distribution is uniform or non-uniform. In the present work, uniform flow distribution was assumed. Object-oriented programming makes it easier to change a model which assumes uniform flow distribution into one which does not, because the equations to describe this phenomenon are only located in the mixture cell due to the modular capability of this programming technique. According to the assumption of uniform flow distribution, any outlet of the mixture cell r has the same conditions, which are calculated with:

$$\dot{m}_{r,\text{out}} = \frac{\sum_1^{n_{r,\text{in}}} \dot{m}_{r,\text{in}}}{n_{r,\text{out}}} \tag{12}$$

$$h_{r,\text{out}} = h_{r,\text{in}} \tag{13}$$

where a mixture cell r is connected to $n_{r,\text{ in}}$ inlet tubes and $n_{r,\text{ out}}$ outlet tubes.

A mixture cell in this kind of heat exchanger would be a portion of a header tube, so there is a pressure drop due to the insertion of the tubes into the header, which can be treated as a sudden expansion or contraction. Additionally, the frictional and gravitational pressure drop along the headers could be evaluated applying Eq. (9) and Eq. (11) to the corresponding mixture cell.

2.2.3. *Fin wall and its thermal connections*

The present model discretizes the fin height, together with the air in contact, into three cells (Fig. 5(b)); two short cells of equal height, which are in contact with the corresponding tubes, and a central cell. The reason for applying this discretization is that in this way, the assumption of uniform temperature along Y direction of the air cell in contact with each fin cell is more correct. In this manner, Eq. (3) can be applied more fundamentally to each fin-air connection than in a situation with just one air cell. Thus, in the proposed model the fin theory is applied to each fin-air connection, which means applying Eq. (3) for each fin cell, resulting in a column of fin cells in the system of Eq. (14). That is the reason for the model's name: 1D because it applies a one-dimensional equation for each fin-air connection and "x3" because it is applied for three connections per fin.

$$\theta_{f,a}(Y) = \begin{cases} \theta_{f,a1}(Y) = C_1\, e^{m_{f,a1} Y} + C_2\, e^{-m_{f,a1} Y}, & 0 \le Y \le \varphi\, H_f \\ \theta_{f,a2}(Y) = C_3\, e^{m_{f,a2}\left(Y-\varphi\, H_f\right)} + C_4\, e^{-m_{f,a2}\left(Y-\varphi\, H_f\right)}, & \varphi\, H_f \le Y \le (1-\varphi) H_f \\ \theta_{f,a3}(Y) = C_5\, e^{m_{f,a3}\left[Y-(1-\varphi)\, H_f\right]} + C_6\, e^{-m_{f,a3}\left[Y-(1-\varphi)\, H_f\right]}, & (1-\varphi) H_f \le Y \le H_f \end{cases} \tag{14}$$

In Eq. (14) H_f is the fin height and φ is the non-dimensional height of fin and air cells at the bottom and top of the fin. Eq. (14) assumes uniform air temperature inside each region, along the Y-Z directions, so to obtain the fin wall temperature (Eq. (15)), an integrated mean value is used for the air temperature, which corresponds to $\overline{T}_a$. Actually this value corresponds to an integrated value along the Z direction since the air temperature for each corresponding region is uniform along the Y direction.

$$T_f(Y) = \begin{cases} T_{f1}(Y) = \theta_{f,a1}(Y) + \overline{T}_{a1}, & 0 \le Y \le \varphi\, H_f \\ T_{f2}(Y) = \theta_{f,a2}(Y) + \overline{T}_{a2}, & \varphi\, H_f \le Y \le (1-\varphi) H_f \\ T_{f3}(Y) = \theta_{f,a3}(Y) + \overline{T}_{a3}, & (1-\varphi) H_f \le Y \le H_f \end{cases} \tag{15}$$

The unknown constants: C_1, C_2, C_3, C_4, C_5, C_6 must be evaluated from the boundary conditions of the heat transfer problem along the fin height, i.e., the temperature field must be continuous and derivable. Therefore, the conditions to evaluate the constants are:

$$\begin{cases} T_{f1}(Y=0) = T_{fB} \\ T_{f1}\left(Y=\varphi H_f\right) = T_{f2}\left(Y=\varphi H_f\right) \\ T_{f3}\left(Y=H_f\right) = T_{fT} \\ T_{f2}\left(Y=(1-\varphi) H_f\right) = T_{f3}\left(Y=(1-\varphi) H_f\right) \\ \left.\dfrac{dT_{f1}}{dY}\right|_{Y=\varphi H_f} = \left.\dfrac{dT_{f2}}{dY}\right|_{Y=\varphi H_f} \\ \left.\dfrac{dT_{f2}}{dY}\right|_{Y=(1-\varphi) H_f} = \left.\dfrac{dT_{f3}}{dY}\right|_{Y=(1-\varphi) H_f} \end{cases} \tag{16}$$

where T_{fB} and T_{fT}, illustrated in Fig. 5(c), correspond to the temperature at the bottom and top of the fin in the base of contact with the bottom and top tube cells, respectively. In this way, it is possible to define T_f as follows,

$$T_f(Y) = \begin{Bmatrix} T_{f1}(Y) \\ T_{f2}(Y) \\ T_{f3}(Y) \end{Bmatrix} = [A(Y)] \begin{Bmatrix} \overline{T}_{a1} \\ \overline{T}_{a2} \\ \overline{T}_{a3} \\ T_{fB} \\ T_{fT} \end{Bmatrix} \tag{17}$$

$[A(Y)]$ is a 3 × 5 matrix that depends on Y, geometry, air-side heat transfer coefficient and fin conductivity, which weakly depend on the temperatures solution. However, as the solving procedure is iterative, it becomes linear when the components of Matrix A are computed with the current available values of the variables, i.e., T_f is a pseudo-linear function with respect to $\overline{T}_a$, T_{fB} and T_{fT}.

Once we have an expression for the fin wall temperature function, the governing equations for the thermal connections between fin and tube (Eqs. (18) and (19)) can be obtained by requiring that the heat conduction at the bottom (Eq. (18)) and top (Eq. (19)) of the fin are equal to the heat conduction, in the Y direction, through the n_t wall tube cells in contact. The conduction areas between a tube cell t and the bottom and top of the fin are A_{J_B} and A_{J_T}, respectively; the corresponding conduction areas for the bottom and top of the fin are A_{fB} and A_{fT}, respectively.

$$\sum_{t}^{n_t} A_{t,J_B} \frac{\partial}{\partial Y}\left(k_{t,J_B} T_t\right)\Big|_{Y=0} = A_{fB} \frac{d}{dY}\left(k_{f1} T_{f1}\right)\Big|_{Y=0} \tag{18}$$

$$\sum_{t}^{n_t} A_{t,J_T} \frac{\partial}{\partial Y}\left(k_{t,J_T} T_t\right)\Big|_{Y=H_f} = A_{fT} \frac{d}{dY}\left(k_{f3} T_{f3}\right)\Big|_{Y=H_f} \tag{19}$$

2.2.4. Air flow

Eq. (20) states the energy conservation in an air cell a in contact with a fin cell f and n_t tube cells $t = 1, n_t$.

$$\dot{m}_a dh_a = d\dot{Q}_{f,a} + \sum_{t=1}^{n_t} \dot{q}_{t,a} P_{t,a} dZ \tag{20}$$

The heat flux $\dot{q}_{t,a}$ exchanged with each tube cell t is calculated by applying Eq. (5), while the heat transferred to the neighbouring fin cell f, can be evaluated by:

$$d\dot{Q}_{f,a} = \alpha_{f,a} P_{f,a} \theta_{f,a} dY \tag{21}$$

The air pressure drop along the fluid cell i length is obtained by applying the momentum equation:

$$\Delta p_a = \Delta p_{a,fr} + \Delta p_{a,acc} + \Delta p_{a,cont} + \Delta p_{a,exp} \tag{22}$$

where $\Delta p_{a,fr}$ and $\Delta p_{a,\,acc}$ are evaluated with Eqs. (9) and (10), respectively. The pressure drop terms due to the sudden contraction and expansion in the heat exchanger are obtained following Kays and London (1984). The different correlations employed to evaluate the heat transfer and pressure drop coefficients are listed in Table 1.

To solve the system of equations, a set of boundary conditions is needed. Inlet conditions and velocity distributions are known for both fluids. Additionally, the heat transferred by the wall edges to the surroundings is usually considered as negligible, so the edges of the extreme wall cells are adiabatic with the surrounding. A real heat exchanger is closed at the bottom and top with two metal plates. In the proposed model, these two metal plates have been modelled as empty tubes, i.e., tubes with the same geometry as the rest, but without refrigerant flowing inside, which are adiabatic with the surrounding.

2.3. Numerical scheme

In order to discretize the governing equations presented in the previous subsection, a finite volume method (FVM) was applied. In the governing equations, the wall temperature has been considered as the iterative variable of the problem, and the semi-explicit method for wall temperature linked equations (SEWTLE) proposed by Corberán et al. (2001) has been employed to solve the problem. The use of the wall temperature as an independent variable gives more freedom to formulate the heat transfer phenomenon, allowing the formulation of equations for energy conservation with fewer assumptions than classical ε-NTU approaches. Additionally, using the wall temperature as an independent variable of the thermal problem converts an implicit problem into a semi-explicit problem, by solving at each iteration a series of explicit steps.

In order to integrate the Laplacian operator in Eq. (6), it has been discretized by a classical finite difference (finite volume) approach.

$$a_t T_t - \sum_{k=W,E,S,N} a_{t,k} T_{t,k} = a_{t,J_B} T_{t,fB} + a_{t,J_T} T_{t,fT} - \sum_{i=1}^{n_i} P_{t,i} U_{t,i} \left(T_t - T_i\right) ds_{t,i} \tag{23}$$

$$a_{t,W} = \frac{k_{t,W} A_{t,W}}{\delta l_{t,W}} \quad a_{t,E} = \frac{k_{t,E} A_{t,E}}{\delta l_{t,E}} \quad a_{t,S} = \frac{k_{t,S} A_{t,S}}{\delta l_{t,S}} \quad a_{t,N} = \frac{k_{t,N} A_{t,N}}{\delta l_{t,N}}$$

$$a_{t,J_B} = \frac{k_{t,J_B} A_{t,J_B}}{\delta l_{t,J_B}} \quad a_{t,J_T} = \frac{k_{t,J_T} A_{t,J_T}}{\delta l_{t,J_T}} \quad a_t = \sum_{k=W,E,S,N,J_B,J_T} a_{t,k}$$

Notice that the term in Eq. (23) of the heat transferred to the fluids in contact is applied to both refrigerant and air cells in contact with a tube cell t. The direction reference used in the model for k is shown in Fig. 5(a). All $a_{t,\,k}$ terms refer to the conductance between a tube cell t and the neighbouring tube cell in the k direction. a_{t,J_B} and a_{t,J_T} are the conductance of the connection between a tube cell t and the correspondent fin base, at either the bottom or the top of each fin respectively.

To continue discretizing the set of governing equations, first it is necessary to assume a temperature profile for the tube walls, or for the fluids, in order to obtain the estimation of the integral of the heat transferred to the fluids in contact with a considered piece of wall (Eqs. (5) and (6)) in the fluid flow direction. This integration must be consistent with the integration of the coincident terms of fluid energy Eqs. (7) and (20).The linear fluid temperature variation scheme (LFTV) has been assumed for both fluids, as Corberán et al. (2001) suggested for this application, leading to the following expression:

$$A_{t,i} \dot{q}_{t,i} = U_{t,i} P_{t,i} \left(T_t - \frac{T_{i,in} + T_{i,out}}{2}\right) \Delta s_{t,i} \tag{24}$$

Eq. (24) is valid for both refrigerant and air cells in contact with a tube cell t. Substituting Eq. (24) in Eq. (23), the tube wall temperature can be evaluated as follows:

$$T_t = \frac{\sum_{k=W,E,S,N} a_{t,k} T_{t,k} + a_{t,J_B} T_{t,fB} + a_{t,J_H} T_{t,fH} + \sum_{i=1}^{n_i} P_{t,i} U_{t,i} 0.5 \left(T_{i,out} + T_{i,in}\right) \Delta s_{t,i}}{a_t + \sum_{i=1}^{n_i} P_{t,i} U_{t,i} \Delta s_{t,i}} \tag{25}$$

By combining Eq. (7) and Eq. (24), the outgoing temperature of a refrigerant cell r, can be expressed by:

$$T_{r,out} = \frac{T_{r,in}\left(1 - 0.5 \sum_{t=1}^{n_t} NTU_{t,r}\right) + \sum_{t=1}^{n_t} NTU_{t,r} T_t}{\left(1 + 0.5 \sum_{t=1}^{n_t} NTU_{t,r}\right)} \tag{26}$$

$$NTU^{t,i} = \frac{P_{t,i} U_{t,i} \Delta s_{t,i}}{\dot{m}_i C p_i}$$

Eq. (26) is used for a one-phase flow, whereas for two-phase flow the outlet temperature depends on the outlet pressure. To obtain the outgoing temperature of the air, Eq. (20) has to be

solved, so the integration of Eq. (21) must be done previously. The total heat transfer along the fin cell can be expressed as:

$$\int d\dot{Q}_{f,a} = \int \alpha_{f,a} P_{f,a} \theta_{f,a} dY = \alpha_{f,a}\, A_{f,a}\, \overline{\theta}_{f,a} \tag{27}$$

where $\overline{\theta}_{f,a}$ is the integrated mean value of $\theta_{f,a}(Y)$. A novel aspect of this model is that in order to include heat transfer from fin to air, integration of temperature difference $\theta_{f,a}$ is implemented in the model, while the rest of the models use directly a fin efficiency by applying the analytical relationship for the adiabatic-fin-tip assumption, tanh(mL)/mL.

The advantage of using the integration of $\theta_{f,a}$ is that allows us to take into account the heat conduction between tubes more easily and fundamentally than other fin efficiency based approaches. Furthermore, a fin efficiency cannot be always be defined, e.g., when temperatures at fin roots are not identical. This fact leads to some models, which use the adiabatic-fin-tip efficiency, applying more or less artificial approaches in order to include heat conduction between tubes. It is important to note that this idea is independent of the discretization applied in air and fin; that is, with just one air cell, instead of three as this paper proposes, applying this idea is possible. Thus, there is neither an accuracy nor a computational cost reason to apply an approach based on the use of an adiabatic-fin-tip efficiency instead of the previous methodology, which is fundamentally more appropriate. Part II (Martínez-Ballester et al., submitted for publication) will present a comparison of the accuracy of the results of both methodologies, when one air and fin cell is used instead of three.

By using Eq. (27), Eq. (20) can be written for each region of the fin in the following way:

$$\begin{Bmatrix} \dot{m}_{a1}\Delta h_{a1} \\ \dot{m}_{a2}\Delta h_{a2} \\ \dot{m}_{a3}\Delta h_{a3} \end{Bmatrix} = \begin{Bmatrix} \alpha_{f,a1} A_{f,a1} \overline{\theta}_{f,a1} \\ \alpha_{f,a2} A_{f,a2} \overline{\theta}_{f,a2} \\ \alpha_{f,a3} A_{f,a3} \overline{\theta}_{f,a3} \end{Bmatrix} + \begin{Bmatrix} \sum_{t=1}^{n_t} \dot{q}_{t,a1} P_{t,a1} \Delta Z_{t,a1} \\ 0 \\ \sum_{t=1}^{n_t} \dot{q}_{t,a3} P_{t,a3} \Delta Z_{t,a3} \end{Bmatrix} \tag{28}$$

The linear fluid temperature variation (LFTV) approach was also assumed for the air, along the Z direction, so the set of Eq. (28) can be rewritten as:

$$\begin{Bmatrix} 2(\overline{T}_{a1} - T_{a1,in}) \\ 2(\overline{T}_{a2} - T_{a2,in}) \\ 2(\overline{T}_{a3} - T_{a3,in}) \end{Bmatrix} = \begin{Bmatrix} NTU_{f,a1} \overline{\theta}_{f,a1} \\ NTU_{f,a2} \overline{\theta}_{f,a2} \\ NTU_{f,a3} \overline{\theta}_{f,a3} \end{Bmatrix} + \begin{Bmatrix} \sum_{t=1}^{n_t} NTU_{t,a1} (T_t - \overline{T}_{a1}) \\ 0 \\ \sum_{t=1}^{n_t} NTU_{t,a3} (T_t - \overline{T}_{a3}) \end{Bmatrix} \tag{29}$$

$$\begin{bmatrix} \frac{2 + \sum_{t=1}^{n_t} NTU_{t,a1}}{NTU_{f,a1}} - B_{1,1} & -B_{1,2} & -B_{1,3} \\ -B_{2,1} & \frac{2}{NTU_{f,a2}} - B_{2,2} & -B_{2,3} \\ -B_{3,1} & -B_{3,2} & \frac{2 + \sum_{t=1}^{n_t} NTU_{t,a3}}{NTU_{f,a3}} - B_{3,3} \end{bmatrix} \cdot \begin{bmatrix} \overline{T}_{a1} \\ \overline{T}_{a2} \\ \overline{T}_{a3} \end{bmatrix} = \begin{bmatrix} \frac{2T_{a1,in} + \sum_{t=1}^{n_t} T_t\, NTU_{t,a1}}{NTU_{f,a1}} + T_{fB} B_{1,4} + T_{fT} B_{1,5} \\ \frac{2T_{a2,in}}{NTU_{f,a2}} + T_{fB} B_{2,4} + T_{fT} B_{2,5} \\ \frac{2T_{a3,in} + \sum_{t=1}^{n_t} T_t\, NTU_{t,a3}}{NTU_{f,a3}} + T_{fB} B_{3,4} + T_{fT} B_{3,5} \end{bmatrix} \tag{32}$$

$$NTU_{f,a} = \frac{\alpha_{f,a} A_{f,a}}{\dot{m}_a Cp_a}$$

where $NTU_{t,a}$ is defined for the thermal connection between a tube cell t and an air cell a, while $NTU_{f,a}$ is defined for the thermal connection between an air cell a and an attached fin cell f.

In Eq. (29) the term $\overline{\theta}_{f,a}$ corresponds to $\overline{T}_f - \overline{T}_a$, whilst $\overline{T}_f$ can be obtained by integration of Eq. (17), resulting in the following equations:

$$\overline{T}_f = \begin{Bmatrix} \overline{T}_{f1} \\ \overline{T}_{f2} \\ \overline{T}_{f3} \end{Bmatrix} = \begin{bmatrix} \frac{\int_{0s}^{\varphi H_f} [A(Y)]_{1,j}}{\varphi H_f} \\ \frac{\int_{\varphi H_f}^{(1-\varphi)H_f} [A(Y)]_{2,j}}{(1-2\varphi)H_f} \\ \frac{\int_{(1-\varphi)H_f}^{H_f} [A(Y)]_{3,j}}{\varphi H_f} \end{bmatrix} \cdot \begin{Bmatrix} \overline{T}_{a1} \\ \overline{T}_{a2} \\ \overline{T}_{a3} \\ T_{fB} \\ T_{fT} \end{Bmatrix} \tag{30}$$

Now, if $\overline{T}_a$ is subtracted from $\overline{T}_f$ and rearranging the result, $\overline{\theta}_{f,a}$ can be expressed as:

$$\begin{Bmatrix} \overline{\theta}_{f,a1} \\ \overline{\theta}_{f,a2} \\ \overline{\theta}_{f,a3} \end{Bmatrix} = \begin{Bmatrix} \overline{T}_{f1} - \overline{T}_{a1} \\ \overline{T}_{f2} - \overline{T}_{a2} \\ \overline{T}_{f3} - \overline{T}_{a3} \end{Bmatrix} = [B] \cdot \begin{Bmatrix} \overline{T}_{a1} \\ \overline{T}_{a2} \\ \overline{T}_{a3} \\ T_{fB} \\ T_{fT} \end{Bmatrix} \tag{31}$$

[B] is a 3 × 5 matrix that depends on the same parameters as [A(Y)] excepting Y. A full description of each term of this matrix is reported in Appendix A. $\overline{\theta}_{f,a}$ depends on the outlet temperatures of all the air cells located at the same Z (of the same segment). However, note that $\overline{\theta}_{f,a}$ has the interesting characteristic, the same as $T_f(Y)$, that is expressed as a pseudo-linear function with respect to $\overline{T}_a$, T_{fB} and T_{fT}. The advantage of using pseudo-linear functions is that it is possible to solve all the proposed equations using a fast iterative method with good convergence.

If Eq. (31) is substituted in Eq. (29), and rearranging, the system of equations to solve is the set of Eq. (32). The average air temperature and consequently the outlet air temperature for each segment are obtained simultaneously by solving the system of Eq. (32). The solution for a system of 3 linear equations is known and easy to compute.

Now, we have to discretize Eqs. (18) and (19) in order to relate temperature at the bottom and top of a fin with the temperature at the corresponding connected tube cells. The

discretization of these equations, attending to the proposed heat exchanger discretization and using some terms of Eq. (23), is:

$$\left\{\begin{array}{l}\sum_{t=1}^{n_t} a_{t,J_B}\left(T_t - T_{fB}\right) = -A_{fB}k_{fB}\left.\dfrac{dT_{f1}}{dY}\right|_{Y=0}\\ \sum_{t=1}^{n_t} a_{t,J_T}\left(T_t - T_{fT}\right) = A_{fT}k_{fT}\left.\dfrac{dT_{f3}}{dY}\right|_{Y=H_f}\end{array}\right\} \tag{33}$$

where the derivative of the temperature at the bottom and top of the fin can be evaluated from Eq. (17), resulting in:

$$\left\{\begin{array}{l}\left.\dfrac{dT_{f1}}{dY}\right|_{Y=0}\\ \left.\dfrac{dT_{f3}}{dY}\right|_{Y=H_f}\end{array}\right\} = [C]\left\{\begin{array}{l}\overline{T}_{a1}\\ \overline{T}_{a2}\\ \overline{T}_{a3}\\ T_{fB}\\ T_{fT}\end{array}\right\} \tag{34}$$

where $[C]$ is obtained by deriving the corresponding rows of $[A(Y)]$ (Eq. (17)) and evaluating them at $Y = 0$ or $Y = H_f$, respectively. A full description of each term of $[C]$ is reported in Appendix A. Substitution of Eq. (34) in Eq. (33) results in the following system of equations:

$$\begin{bmatrix}\left(C_{1,4} - \sum_{t=1}^{n_t}\chi_{t,B}\right) & C_{1,5}\\ -C_{2,4} & -\left(\sum_{t=1}^{n_t}\chi_{t,T} + C_{2,5}\right)\end{bmatrix}\cdot\begin{bmatrix}T_{fB}\\ T_{fT}\end{bmatrix} = \begin{bmatrix}-C_{1,1}\overline{T}_{a1} - C_{1,2}\overline{T}_{a2} - C_{1,3}\overline{T}_{a3} - \sum_{t=1}^{n_t}\chi_{t,B}T_t\\ C_{2,1}\overline{T}_{a1} + C_{2,2}\overline{T}_{a2} + C_{2,3}\overline{T}_{a3} - \sum_{t=1}^{n_t}\chi_{t,T}T_t\end{bmatrix} \tag{35}$$

where the following expressions have been used, for the thermal conductance at the bottom and top of the fin:

$$\chi_{t,B} = \frac{a_{t,J_B}}{A_{fB}k_{fB}}, \quad \chi_{t,T} = \frac{a_{t,J_T}}{A_{fT}k_{fT}}$$

This system is again a linear system of equations, and it is employed to relate T_{fB} and T_{fT} with $\overline{T}_a$ and T_t.

At this point, all the equations which describe the thermal problem have been discretized. The pressure drop equations, presented earlier in Subsection 2.2, were already in discretized form.

To summarize, the proposed model applies to each segment of Equations (25), (26), (32) and (35), with T_{fB}, T_{fT}, T_t, $T_{r,out}$ and $T_{a,out}$ being the unknown variables of the problem for each of the cells of the heat exchanger. Once these variables are known, any performance parameter of the heat exchanger can be calculated, including the fin temperature at any position Y by means of Eq. (17).

2.4. *Solution methodology*

The global solution method is based on the SEWTLE method, outlined by Corberán et al. (2001), with some differences due to the particularities of the present model.

The proposed system of equations consists of a system of non-linear equations, since coefficients and properties depend on the temperature and pressure field. The functions of the properties and coefficients are strongly non-linear and too complex to introduce directly in the system of equations. Thus, the solution needs an iterative process. A first option could be to start solving the problem assuming constant coefficients and properties. Corberán et al. (2001) concluded that it is not worth finding the exact solution for such a system, since even with the exact solution the properties/coefficients have to be recalculated and the system must be solved again and again. They proposed that a better strategy would be to "*combine the iterative calculation of the solution with the continuous updating of the coefficients, in such a way that both calculations progress together toward the solution of the nonlinear problem*". The proposed numerical scheme fits quite well with this strategy, since it consists of a set of explicit equations.

The solution methodology applied in the present work is summarized in Fig. 6. In the first step, the fluid outlet temperatures in each cell are initialized, for both fluids, with the corresponding inlet temperature. Each wall cell is initialized using the average temperature of the fluid cells in contact with it. Since the temperatures at the bottom and top of the fin are required, these temperatures are initialized with the same value as that adopted for the attached tube cells.

The first step in the iterative procedure is to calculate the fluid outlet temperature for both streams: refrigerant and air.

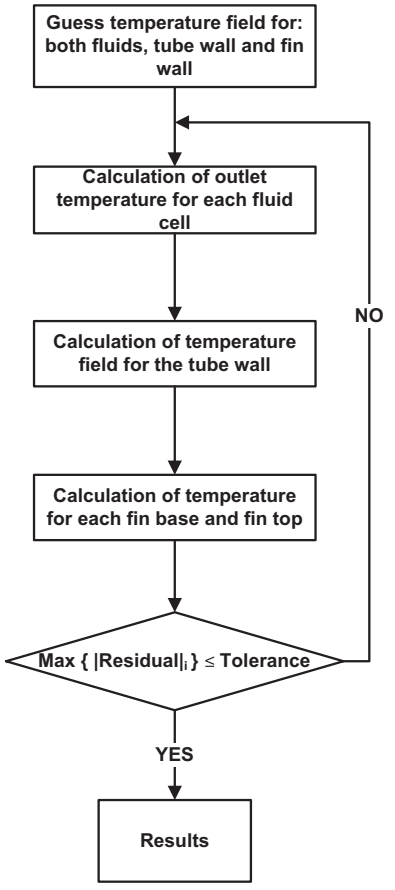

Fig. 6 – Solution methodology for solving the problem.

First, Eq. (26) is used to obtain the refrigerant field temperature. Secondly, for the air flow, the solution of Eq. (32) gives the outlet temperature of each air cell along the height of a fin. Although Eq. (32) represents a system of three equations, note that the solution for such a system is known, and can be easily expressed as an explicit equation for each air cell, so that it is not necessary to solve numerically the inverse matrix of Eq. (32). Thus, the outlet temperatures of the three air cells of each fin column (in a segment) are obtained explicitly.

Once the fluid temperature has been evaluated in each cell, Eq. (25) must be solved for the tube wall temperature. Note that in this step the temperature field of fluids and the fin bottom and fin top temperatures are known. In the presence of LHC, Eq. (25) shows that the wall temperature of a wall cell t depends on the wall temperature of the neighbouring wall cells. When there is no LHC the exact solution, at this step, consists of explicit calculations.

In the case of LHC being present, it is necessary to solve a system of linear equations, involving all the tube cell temperatures. If we take into account that it is not worth obtaining the exact solution in each step, as was explained above, the best methodologies to deal with this calculation are:

- Using for each tube cell equation the values of the temperature of neighbouring tube cells corresponding to the previous iteration. This converts Eq. (25) into an explicit equation, but this method will increase considerably the time to reach the convergence.
- The line-by-line iteration method (Patankar, 1980). Due to the characteristics of the system, it converts the system of equations into a tridiagonal system of equations, which is easily solved. When the LHC is in only one direction, this methodology gives the exact solution.
- Block-by-block (Patankar, 1980). This is based on the line-by-line method, but it adds a correction to the solution after finishing each iteration. It has the advantage of a faster convergence than the line-by-line method but it needs twice the number of operations.

Regardless of the selected methodology, this step calculates the wall tube temperature field by means of a set of explicit calculations. In particular, these calculations will be the exact solution in the case that no LHC is present or when LHC is present only in the tube along one direction and the line-by-line method is used.

The last step consists of solving the temperature field for the fin wall cells at the bottom and top of the fins. For each fin, both temperatures are obtained from Eq. (35). This system has only two equations and the solution can be easily expressed as two explicit equations. Note that because there is no longitudinal heat conduction in the fin along the Z direction, the fin wall temperature field does not need an iterative resolution, as was the case in the Fin2D model, so that the process to obtain the fin wall temperature field results is explicit. An interesting point of the fin discretization is that though the fin wall is discretized into three cells, computationally it behaves as just one fin cell. In fact, the total number of unknown variables for each fin, regardless of the number of fin cells is two: the temperatures at the fin and the bottom of the fin.

3. Model validation

In order to validate the proposed model, a set of existing experimental results are going to be compared with the thermal capacity predicted by the model, when inlet conditions and mass flow rates are provided for both fluids. The model is able to simulate both gas cooler and condenser, so both scenarios are validated.

The grid size chosen was the one that gave a good balance between accuracy and computational cost. According to the definition given in Subsection 2.1, the grid employed for all the predicted results was: {5,1,3,3}. The authors (Martínez-Ballester et al., 2011) previously studied the effect of simulating the actual number of channels or just one channel with an identical hydraulic diameter, and they concluded that the differences were negligible. Therefore, regardless of the actual number of channels per tube, only a hydraulic equivalent channel was modelled.

The fin height ratio φ, has still not been evaluated. This parameter could be adjusted experimentally, numerically or even by observation. According to the corresponding explanations in Section 2, it is possible to get a first approach from: typical dimensions of louvered fins used in this type of heat exchangers; the value reported by Martínez-Ballester et al. (2011) was about 3%. Thus, a value of φ equal to 4% was assumed for the validation and for the different scenarios studied in Part II (Martínez-Ballester et al., submitted for publication). At the end of this section, a simulation study was carried out in order to analyse the influence of this parameter on the solution.

3.1. *Microchannel condenser validation*

The experimental data used was measured by García-Cascales et al. (2010). They measured two condenser arrangements (one-row and two-row) for two refrigerants (R410A and R134a), but for the present work only the experimental data corresponding to the one-row condenser is used for the model's validation. For this arrangement, two condensers working with R410A were tested and have been simulated; their main geometry is described in Table 2. The differences between the two condensers are mainly the number of tubes, the finned length and therefore the capacity.

Fig. 7 presents the predicted capacity against the whole set of experimental values, for both condensers. The model agrees well with the measured capacity and errors are within an error band of ±5%.

In order to obtain these results an adjustment factor of 1.15 was applied to the air-side heat transfer coefficient obtained with the corresponding correlation of Table 1. The main reason for using this factor is related to the use of an empirical correlation for evaluation of the air-side heat transfer coefficient. The correlation may not fit well when the tubes and fins arrangement is different from that used to work out the correlation. The correlation used for the air-side heat transfer coefficient (Kim and Bullard, 2002) reported rms errors of

Table 2 – Geometric characteristics of the condensers used for the model validation (García-Cascales et al., 2010).

Condenser #1			
Face area (cm^2)	1604	Refrigerant side area (m^2)	1.16
Airside area (m^2)	3.9	Tubes number	33
Tube length (mm)	483	Refrigerant passes	4
Fin type	Louvered	Tube depth (mm)	19
Number of ports	19	Fin depth (mm)	21.5
Wall thickness (mm)	0.32	Fin density (fins/in)	14
Hydraulic diameter (mm)	1.276	Fin height (mm)	8.1
Fin thickness (mm)	0.11		
Condenser #2			
Face area (cm^2)	5939	Refrigerant side area (m^2)	3.76
Airside area (m^2)	16.51	Tubes number	66
Tube length (mm)	889	Refrigerant passes	2
Fin type	Louvered	Tube depth (mm)	19
Number of ports	19	Fin depth (mm)	21.5
Wall thickness (mm)	0.32	Fin density (fins/in)	14
Hydraulic diameter (mm)	1.276	Fin height (mm)	8.1
Fin thickness (mm)	0.11		

14.5% for the Colburn factor. Another parameter that affects the prediction results is the φ factor, which has been chosen by observation. The next subsection will assess the influence of this parameter on the predicted results. The authors determined it suitable to use an adjustment factor of 15% for the air-side heat transfer to take into account all the deviations explained above.

The predicted pressure losses of refrigerant were substantially underestimated with regard to the experimental data, with mean errors of 50% and 75% for condenser #1 and condenser #2 respectively. Microchannel tube geometry is hard to measure accurately since small manufacturing uncertainties produce large geometry variations, especially in sub-millimetre port diameters, and thus also pressure losses variations. A different mean error for both condensers also supports this idea. Manufacturing defects, e.g., blocked ports, are also a source of the disagreement in the pressure drop. Yin et al. (2000) reported for an MCHX the average port diameter to be 94% of nominal, and that 39% of ports were blocked.

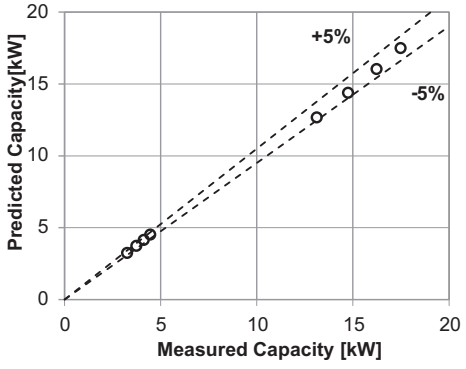

Fig. 7 – Model validation for two condensers by means of comparison between experimental data against predicted capacity.

3.2. *Microchannel gas cooler validation*

The experimental data used corresponds to a CO_2 gas cooler tested by Yin et al. (2001), who measured the performance of the gas cooler over a wide range of operating conditions. The uncertainty for the capacity measurement in those experiments was ±5%. The gas cooler modelled is a parallel tube MCHX of three refrigerant passes, whose main geometric data is summarized in Table 3.

Fig. 8(a) presents the predicted gas cooler capacity against the whole set of experimental values. As can be observed, all the predicted values are within the error bound of ±5%. The accuracy is quite high since a linear function fitted to the predicted capacity had a slope of 0.997, which represents an error of −0.28%, for the whole set of experimental data. For this scenario, no adjustment factor was applied to the heat transfer coefficients.

The outlet refrigerant temperature was also compared against experimental data in Fig. 8(b). The figure includes the bounds of ±2 K around the measured temperatures. As can be observed, all the points deviate from the experimental data by less than ±2 K.

The predicted pressure losses of refrigerant were far from the experimental data, with a mean error of −80%. These errors are similar to those errors reported by Asinari et al. (2004) and Yin et al. (2001) when they evaluated this error with their own models for the same cases. Yin et al. (2001) solve this disagreement by introducing some dimensional changes in ports produced with manufacturing defects. Asinari et al. (2004) demonstrate that by introducing arbitrary multiplying factors, pressure losses agreed well, with a negligible effect on the capacity results. They argue that the reason for the disagreement between the predicted and experimental pressure drop is based on underestimation of the pressure losses when traditional correlations are used for this particular geometry and conditions.

3.3. *Impact of parameter φ on predicted capacity*

The meaning of the fin height ratio φ in the model has been discussed in Section 2 whilst its estimation has been discussed in both Sections 2 and 3. A value of 4% was finally proposed for the validation cases, even though this value depends on the fin surface and operating conditions. To this end, the authors carried out a numerical study about the

Table 3 – Geometric characteristics of gas cooler (Yin et al., 2001).

Face area (cm^2)	1950	Refrigerant side area (m^2)	0.49
Airside area (m^2)	5.2	Tubes number	34
Tube length (mm)	545	Refrigerant passes	3
Fin type	Louvered	Core depth (mm)	16.5
Number of ports	11	Fin density (fins/in)	22
Wall thickness (mm)	0.43	Port diameter (mm)	0.79
Fin thickness (mm)	0.1	Fin height (mm)	8.89

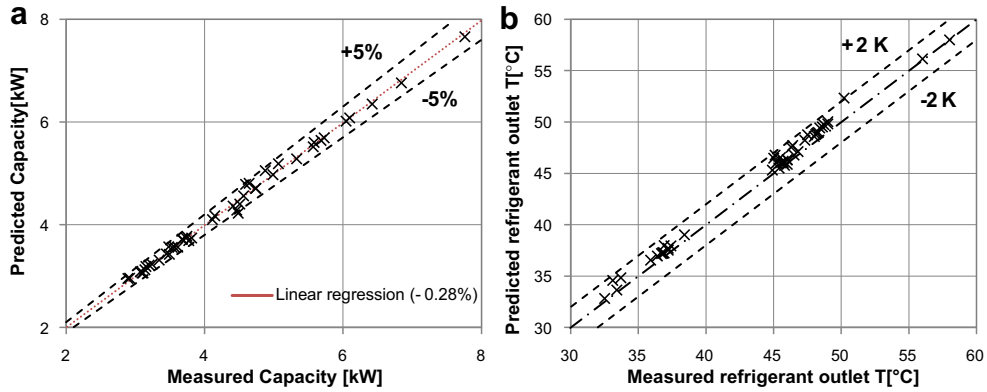

Fig. 8 – Model validation for a gas cooler by means of comparison between experimental data against (a) predicted capacity; (b) predicted refrigerant outlet temperature.

impact of φ on the model results in order to analyse the model's sensitivity to this parameter, which implicitly means the impact of unmixed air flow along Y direction.

The scenario chosen for this study corresponds to the gas cooler introduced earlier in subsection 3.2 working in the operating conditions of test #2 (Yin et al., 2001), which has the largest capacity of all the tests.

Fig. 9 shows the deviation between the heat exchanged by the gas cooler when the parameter φ is modified, with respect to the heat exchanged when φ tends to be 50%. This study is carried out for two fin densities: 22 fpi and 14 fpi. The variation of φ ranges between two limit situations: 0% and 50%. A value close to 50% means that air flow has a temperature profile corresponding to a mixed air flow along the fin height. In fact, for this φ value, if the temperatures of the tubes attached to the fin are identical, air flow has a uniform temperature along the whole fin height. The opposite behaviour is when the φ tends to be 0%, which means that the non-mixed air along the Y direction has the maximum effect. In this situation, a thin air layer is in contact with each tube wall. These air layers have a quite different temperature from the rest of the air because the air flow rate in these cells is very small and its temperature will be very close to the tube wall temperature. Therefore, these air layers will have an insulating effect on the tube wall in contact. Neither situation is real and what actually happens is somewhere between the two.

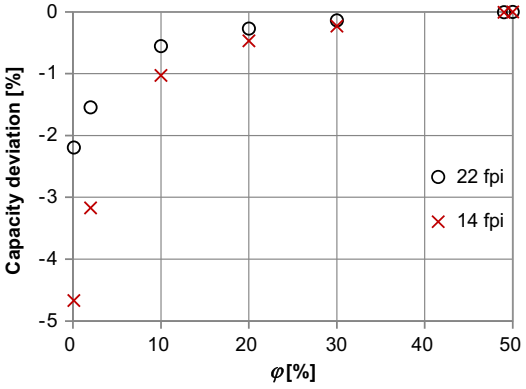

Fig. 9 – Influence of fin height ratio φ on the gas cooler capacity for different fin densities.

The effects described above for extreme values of φ agree quite well with the trend shown in Fig. 9; the lower the φ value, the less capacity is exchanged by the gas cooler. It is interesting to note that the trend is asymptotic for large φ values, whereas the effect of φ changes sharply for low φ values. Louvered fins would have low φ values, while they would be much greater for plain fins. Fig. 9 also shows that impact of φ on the solution depends on the fin density, resulting in values from 2% to 5% for fin densities of 22 fpi and 14 fpi respectively.

This parameter is actually unknown, but fortunately the deviation in predicted capacity would be less than 5% for the fin densities evaluated.

4. Conclusions

The objective of the present work was to develop a model that could reduce significantly the computational cost of the Fin2D model while retaining its accuracy. In this way, it is possible to use that model to analyse microchannel condensers and gas coolers with any refrigerant circuitry, including serpentine heat exchangers.

Part I focussed on the description of governing equations, the numerical scheme and experimental validation of the model. The main conclusion is that it is possible to take into account the heat conduction between tubes in a more fundamental way than other fin efficiency based approaches, which have to apply heat conduction terms to an approach that uses the adiabatic-fin-tip assumption, which is not satisfied in such cases. The alternative methodology, proposed in this work, consists in evaluating the heat transfer by integration of the corresponding fin temperature profile instead of using a fin efficiency which cannot always be defined, e.g., when temperatures at fin roots are different. It has been shown that this integration does not represent an obstacle since it can be easily discretized consistently with the rest of the governing equations; therefore there is neither an

accuracy nor a computational cost reason to apply the adiabatic-fin-tip assumption when it is not satisfied. The approach proposed in this paper is developed for a three air-fin cells discretization, but this conclusion is equally applicable to a single air-fin discretization.

The remaining conclusions that can be drawn from Part I are the following:

- The Fin1Dx3 model accounts for all the same effects as the Fin2D model except for the LHC in the fin along the Z direction which, in any case, has been found to be unimportant. Fin1Dx3 is based on a novel discretization methodology for the air and fin wall that only needs three air cells along the Y direction, which allows a drastic reduction of the number of cells to compute compared with the Fin2D model, and consequently of the simulation time, while keeping a high resolution along the Y direction.
- The large number of fin cells needed by the Fin2D model to solve accurately the air-side heat transfer, is compensated in Fin1Dx3 with a novel methodology to describe the air-side heat transfer, using a composed function for the fin temperature. This composed function, together with the employed air discretization, allows the application in a more fundamental way of the fin analytical solution.
- The main capabilities of Fin1Dx3 are: 2D-LHC in the tube wall; non-mixed air effects due to the temperature difference between bulk air and the air close to the tubes; and it accounts fundamentally for heat conduction between tubes since it does not apply the adiabatic-fin-tip assumption.
- The equations have been discretized, with the interesting characteristic of resulting in a system of pseudo-linear equations with respect to the variables of the problem. A numerical scheme has been proposed to solve the problem as a series of explicit steps. The numerical scheme proposed allows computation of the three fin cells with the computational effort of just one fin cell.
- The Fin1Dx3 model was validated with experimental data, for both condenser and gas cooler. The predicted capacity is within ±5% error, being much more accurate for the gas cooler scenario. Although the pressure drop was drastically underpredicted, it did not affect the heat transfer results.
- The study about the influence on the solution of the factor φ, which accounts for the effects of unmixed air flow along the Y direction, showed deviations less than 5% for extreme values of φ and for the simulated conditions.

Acknowledgements

The first author's work on this project was partially supported by the Ministry for Education of Spain, under the training for university professors program (FPU). Financial support from the Ministry for Education of Spain, project numbers: DPI2008-06707-C02-01 and DPI2011-26771-C02-01, is also gratefully acknowledged. Santiago Martínez-Ballester gratefully acknowledges the National Institute of Standards and Technology, where this work was partially developed and funded, and especially Dr. Piotr A. Domanski for hosting Santiago at NIST as well as for giving his valuable time and advice.

Appendix A

This appendix shows both the matrix [B] and [C] that were obtained and used in the description of the model: Equations (31), (32), (34) and (35).

A.1. Components of $B_{1,j}$

$$B_{1,1} = -\Big(\big(-1+e^{\varphi H_f m_{a1}}\big)\big(e^{\varphi H_f (m_{a1}+4m_{a2}+2m_{a3})}(m_{a1}-2m_{a2})\,(m_{a2}-m_{a3}) + e^{2H_f m_{a2}}(-m_{a1}+2m_{a2})(m_{a2}-m_{a3}) - e^{\varphi H_f m_{a1}+2H_f m_{a2}}(m_{a1}+2m_{a2})(m_{a2}-m_{a3}) + e^{2\varphi H_f (2m_{a2}+m_{a3})}(m_{a1}+2m_{a2})(m_{a2}-m_{a3}) - e^{\varphi H_f (m_{a1}+4m_{a2})}(m_{a1}-2\,m_{a2})(m_{a2}+m_{a3}) - e^{2\,H_f (m_{a2}+\varphi m_{a3})}(-m_{a1}+2\,m_{a2})(m_{a2}+m_{a3}) - e^{4\varphi H_f m_{a2}}(m_{a1}+2\,m_{a2})(m_{a2}+m_{a3}) + e^{H_f (2\,m_{a2}+\varphi(m_{a1}+2\,m_{a3}))}(m_{a1}+2m_{a2})(m_{a2}+m_{a3})\big)\Big)\Big/\big(\varphi H_f m_{a1}\big(e^{2\varphi H_f (m_{a1}+2m_{a2}+m_{a3})}(m_{a1}-m_{a2})(m_{a2}-m_{a3}) + e^{2H_f m_{a2}}(-m_{a1}+m_{a2})(m_{a2}-m_{a3}) - e^{2H_f (\varphi m_{a1}+m_{a2})}(m_{a1}+m_{a2})(m_{a2}-m_{a3}) + e^{2\varphi H_f (2m_{a2}+m_{a3})}(m_{a1}+m_{a2})(m_{a2}-m_{a3}) - e^{2\varphi H_f (m_{a1}+2\,m_{a2})}(m_{a1}-m_{a2})(m_{a2}+m_{a3}) - e^{2\,H_f (m_{a2}+\varphi m_{a3})}(-m_{a1}+m_{a2})(m_{a2}+m_{a3}) - e^{4\varphi H_f m_{a2}}(m_{a1}+m_{a2})(m_{a2}+m_{a3}) + e^{2H_f (m_{a2}+\varphi(m_{a1}+m_{a3}))}(m_{a1}+m_{a2})(m_{a2}+m_{a3})\big)\big)$$

$$B_{1,2} = \Big(\big(-1+e^{\varphi H_f m_{a1}}\big)^2\big(e^{H_f m_{a2}} - e^{2\varphi H_f m_{a2}}\big)m_{a2}\big(e^{2\varphi H_f (m_{a2}-m_{a3})}(m_{a2}-m_{a3}) + e^{H_f m_{a2}}(-m_{a2}+m_{a3}) - e^{2\varphi H_f m_{a2}}(m_{a2}+m_{a3}) + e^{H_f (m_{a2}-2\varphi m_{a3})}(m_{a2}+m_{a3})\big)\Big)\Big/\big(\varphi H_f m_{a1}\big(e^{2\varphi H_f (m_{a1}-2\,m_{a2}-m_{a3})}(m_{a1}-m_{a2})\,(m_{a2}-m_{a3}) + e^{2\,H_f m_{a2}}(-m_{a1}+m_{a2})(m_{a2}-m_{a3}) - e^{2\,H_f (\varphi m_{a1}-m_{a2})}(m_{a1}+m_{a2})(m_{a2}-m_{a3}) + e^{2\varphi H_f (2\,m_{a2}-m_{a3})}(m_{a1}+m_{a2})(m_{a2}-m_{a3}) - e^{2\varphi H_f (m_{a1}-2\,m_{a2})}(m_{a1}-m_{a2})(m_{a2}+m_{a3}) - e^{2\,H_f (m_{a2}-\varphi m_{a3})}(-m_{a1}+m_{a2})(m_{a2}+m_{a3}) - e^{4\varphi H_f m_{a2}}(m_{a1}+m_{a2})(m_{a2}+m_{a3}) + e^{2\,H_f (m_{a2}-\varphi(m_{a1}-m_{a3}))}(m_{a1}+m_{a2})(m_{a2}+m_{a3})\big)\big)\big)$$

$$B_{1,3} = \Big(\Big(2e^{(1+2\varphi)H_f m_{a2}}\big(-1+e\varphi H_f m_{a1}\big)^2\big(-1+e^{\varphi H_f m_{a3}}\big)^2 m_{a2}m_{a3}\Big)\Big/\big(\varphi H_f m_{a1}\big(e^{2\varphi H_f (m_{a1}+2\,m_{a2}+m_{a3})}(m_{a1}-m_{a2})(m_{a2}-m_{a3}) + e^{2\,H_f m_{a2}}(-m_{a1}+m_{a2})\,(m_{a2}-m_{a3}) - e^{2\,H_f (\varphi m_{a1}+m_{a2})}(m_{a1}+m_{a2})(m_{a2}-m_{a3}) + e^{2\varphi H_f (2m_{a2}+m_{a3})}(m_{a1}+m_{a2})(m_{a2}-m_{a3}) - e^{2\varphi H_f (m_{a1}+2\,m_{a2})}(m_{a1}-m_{a2})\,(m_{a2}+m_{a3}) - e^{2\,H_f (m_{a2}+\varphi m_{a3})}(-m_{a1}+m_{a2})\,(m_{a2}+m_{a3}) - e^{4\varphi H_f m_{a2}}(m_{a1}+m_{a2})(m_{a2}+m_{a3}) + e^{2\,H_f (m_{a2}+\varphi(m_{a1}+m_{a3}))}(m_{a1}+m_{a2})(m_{a2}+m_{a3})\big)\big)\Big)$$

$$B_{1,4} = \left(\left(-1+e^{\varphi H_f m_{a1}}\right)\left(e^{\varphi H_f (m_{a1}+4\,m_{a2}+2\,m_{a3})}(m_{a1}-m_{a2})(m_{a2}-m_{a3}) + e^{2\,H_f m_{a2}}(-m_{a1}+m_{a2})(m_{a2}-m_{a3}) - e^{\varphi H_f m_{a1}+2\,H_f m_{a2}}(m_{a1}+m_{a2})(m_{a2} - m_{a3}) + e^{2\varphi H_f (2\,m_{a2}+m_{a3})}(m_{a1}+m_{a2})(m_{a2}-m_{a3}) - e^{\varphi H_f (m_{a1}+4\,m_{a2})}(m_{a1}-m_{a2})(m_{a2}+m_{a3}) - e^{2\,H_f (m_{a2}+\varphi m_{a3})}(-m_{a1}+m_{a2})(m_{a2}+m_{a3}) - e^{4\varphi H_f m_{a2}}(m_{a1}+m_{a2})(m_{a2}+m_{a3}) + e^{H_f (2\,m_{a2}+\varphi(m_{a1}+2\,m_{a3}))}(m_{a1}+m_{a2})(m_{a2}+m_{a3})\right)\right)\Big/\left(\varphi H_f m_{a1}\left(e^{2\varphi H_f (m_{a1}+2\,m_{a2}+m_{a3})}(m_{a1}-m_{a2})(m_{a2}-m_{a3}) + e^{2\,H_f m_{a2}}(-m_{a1}+m_{a2})(m_{a2}-m_{a3}) - e^{2\,H_f (\varphi m_{a1}+m_{a2})}(m_{a1}+m_{a2})(m_{a2}-m_{a3}) + e^{2\varphi H_f (2\,m_{a2}+m_{a3})}(m_{a1}+m_{a2})(m_{a2}-m_{a3}) - e^{2\varphi H_f (m_{a1}+2\,m_{a2})}(m_{a1}-m_{a2})(m_{a2}+m_{a3}) - e^{2\,H_f (m_{a2}+\varphi m_{a3})}(-m_{a1}+m_{a2})(m_{a2}+m_{a3}) - e^{4\varphi H_f m_{a2}}(m_{a1}+m_{a2})(m_{a2}+m_{a3}) + e^{2\,H_f (m_{a2}+\varphi(m_{a1}+m_{a3}))}(m_{a1}+m_{a2})(m_{a2}+m_{a3}))\right)$$

$$B_{1,5} = \left(\left(4\,e^{H_f (m_{a2}+2\varphi m_{a2}+\varphi m_{a3})}\left(-1+e^{\varphi H_f m_{a1}}\right)^2 m_{a2} m_{a3}\right)\Big/\left(\varphi H_f m_{a1}\left(e^{2\varphi H_f (m_{a1}+2\,m_{a2}+m_{a3})}(m_{a1}-m_{a2})(m_{a2}-m_{a3}) + e^{2\,H_f m_{a2}}(-m_{a1}+m_{a2})(m_{a2} - m_{a3}) - e^{2\,H_f (\varphi m_{a1}+m_{a2})}(m_{a1}+m_{a2})(m_{a2}-m_{a3}) + e^{2\varphi H_f (2\,m_{a2}+m_{a3})}(m_{a1}+m_{a2})(m_{a2}-m_{a3}) - e^{2\varphi H_f (m_{a1}+2\,m_{a2})}(m_{a1}-m_{a2})(m_{a2}+m_{a3}) - e^{2\,H_f (m_{a2}+\varphi m_{a3})}(-m_{a1}+m_{a2})(m_{a2}+m_{a3}) - e^{4\varphi H_f m_{a2}}(m_{a1}+m_{a2})(m_{a2}+m_{a3}) + e^{2\,H_f (m_{a2}+\varphi(m_{a1}+m_{a3}))}(m_{a1}+m_{a2})(m_{a2}+m_{a3}))\right)\right)$$

A.2. Components of $B_{2,j}$

$$B_{2,1} = -\left(\left(-1+e^{\varphi H_f m_{a1}}\right)^2\left(e^{H_f m_{a2}} - e^{2\varphi H_f m_{a2}}\right) m_{a1}\left(e^{2\varphi H_f (m_{a2}+m_{a3})}(m_{a2}-m_{a3}) + e^{H_f m_{a2}}(-m_{a2}+m_{a3}) - e^{2\varphi H_f m_{a2}}(m_{a2}+m_{a3}) + e^{H_f (m_{a2}+2\varphi m_{a3})}(m_{a2} + m_{a3})\right)\right)\Big/\left((-1+2\varphi)\,H_f m_{a2}\left(e^{2\varphi H_f (m_{a1}+2\,m_{a2}+m_{a3})}(m_{a1}-m_{a2})(m_{a2}-m_{a3}) + e^{2\,H_f m_{a2}}(-m_{a1}+m_{a2})(m_{a2}-m_{a3}) - e^{2\,H_f (\varphi m_{a1}+m_{a2})}(m_{a1} + m_{a2})(m_{a2}-m_{a3}) + e^{2\varphi H_f (2\,m_{a2}+m_{a3})}(m_{a1}+m_{a2})(m_{a2}-m_{a3}) - e^{2\varphi H_f (m_{a1}+2\,m_{a2})}(m_{a1}-m_{a2})(m_{a2}+m_{a3}) - e^{2\,H_f (m_{a2}+\varphi m_{a3})}(-m_{a1}+m_{a2}) \times (m_{a2}+m_{a3}) - e^{4\varphi H_f m_{a2}}(m_{a1}+m_{a2})(m_{a2}+m_{a3}) + e^{2\,H_f (m_{a2}+\varphi(m_{a1}+m_{a3}))}(m_{a1}+m_{a2})(m_{a2}+m_{a3}))\right)$$

$$B_{2,2} = \left(\left(\left(e^{H_f m_{a2}} - e^{2\varphi H_f m_{a2}}\right) + e^{2\varphi H_f (m_{a1}+m_{a2}+m_{a3})}(m_{a1}(m_{a2}-2\,m_{a3}) + m_{a2}m_{a3}) + e^{H_f (2\varphi m_{a1}+m_{a2})}(-m_{a1}m_{a2} + 2m_{a1}m_{a3} + m_{a2}m_{a3}) + e^{2\varphi H_f (m_{a1}+m_{a2})}(m_{a2}m_{a3} - m_{a1}(m_{a2}+2\,m_{a3})) + e^{H_f (m_{a2}+2\varphi m_{a3})}(-m_{a2}m_{a3} + m_{a1}(m_{a2}+2\,m_{a3})) - e^{2\varphi H_f m_{a2}}(m_{a2}m_{a3} + m_{a1}(m_{a2}+2\,m_{a3})) + e^{H_f (m_{a2}+2\varphi(m_{a1}+m_{a3}))}(m_{a2}m_{a3} + m_{a1}(m_{a2}+2\,m_{a3}))\right)\Big/\left((-1+2\varphi)H_f m_{a2}\left(e^{2\varphi H_f (m_{a1}+2\,m_{a2}+m_{a3})}(m_{a1}-m_{a2})(m_{a2}-m_{a3}) + e^{2\,H_f m_{a2}}(-m_{a1} + m_{a2})(m_{a2}-m_{a3}) - e^{2\,H_f (\varphi m_{a1}+m_{a2})}(m_{a1}+m_{a2})(m_{a2}-m_{a3}) + e^{2\varphi H_f (2\,m_{a2}+m_{a3})}(m_{a1}+m_{a2})(m_{a2}-m_{a3}) - e^{2\varphi H_f (m_{a1}+2\,m_{a2})}(m_{a1}-m_{a2})(m_{a2} + m_{a3}) - e^{2\,H_f (m_{a2}+\varphi m_{a3})}(-m_{a1}+m_{a2})(m_{a2}+m_{a3}) - e^{4\varphi H_f m_{a2}}(m_{a1}+m_{a2})(m_{a2}+m_{a3}) + e^{2\,H_f (m_{a2}+\varphi(m_{a1}+m_{a3}))}(m_{a1}+m_{a2})(m_{a2}+m_{a3}))\right)\right)$$

$$B_{2,3} = \left(-\left(\left(e^{H_f m_{a2}} - e^{2\varphi H_f m_{a2}}\right)\left(-1+e^{\varphi H_f m_{a3}}\right)^2\left(e^{H_f m_{a2}}(m_{a1}-m_{a2}) + e^{2\varphi H_f (m_{a1}+m_{a2})}(-m_{a1}+m_{a2}) - e^{2\varphi H_f m_{a2}}(m_{a1}+m_{a2}) + e^{H_f (2\varphi m_{a1}+m_{a2})}(m_{a1} + m_{a2})\right)m_{a3}\right)\Big/\left((-1+2\varphi)\,H_f m_{a2}\left(e^{2\varphi H_f (m_{a1}+2\,m_{a2}+m_{a3})}(m_{a1}-m_{a2})(m_{a2}-m_{a3}) + e^{2\,H_f m_{a2}}(-m_{a1}+m_{a2})(m_{a2}-m_{a3}) - e^{2\,H_f (\varphi m_{a1}+m_{a2})}(m_{a1} + m_{a2})(m_{a2}-m_{a3}) + e^{2\varphi H_f (2\,m_{a2}+m_{a3})}(m_{a1}+m_{a2})(m_{a2}-m_{a3}) - e^{2\varphi H_f (m_{a1}+2\,m_{a2})}(m_{a1}-m_{a2})(m_{a2}+m_{a3}) - e^{2\,H_f (m_{a2}+\varphi m_{a3})}(-m_{a1}+m_{a2}) \times (m_{a2}+m_{a3}) - e^{4\varphi H_f m_{a2}}(m_{a1}+m_{a2})(m_{a2}+m_{a3}) + e^{2\,H_f (m_{a2}+\varphi(m_{a1}+m_{a3}))}(m_{a1}+m_{a2})(m_{a2}+m_{a3}))\right)\right)$$

$$B_{2,4} = \left(-\left(2\,e^{\varphi H_f m_{a1}}\left(e^{H_f m_{a2}} - e^{2\varphi H_f m_{a2}}\right)m_{a1}\left(e^{2\varphi H_f (m_{a2}+m_{a3})}(m_{a2}-m_{a3}) + e^{H_f m_{a2}}(-m_{a2}+m_{a3}) - e^{2\varphi H_f m_{a2}}(m_{a2}+m_{a3}) + e^{H_f (m_{a2}+2\varphi m_{a3})}(m_{a2}+m_{a3})\right)\right)\Big/\left((-1+2\varphi)H_f m_{a2}\left(e^{2\varphi H_f (m_{a1}+2\,m_{a2}+m_{a3})}(m_{a1}-m_{a2})(m_{a2}-m_{a3}) + e^{2\,H_f m_{a2}}(-m_{a1}+m_{a2})(m_{a2}-m_{a3}) - e^{2\,H_f (\varphi m_{a1}+m_{a2})}(m_{a1}+m_{a2})(m_{a2}-m_{a3}) + e^{2\varphi H_f (2\,m_{a2}+m_{a3})}(m_{a1}+m_{a2})(m_{a2}-m_{a3}) - e^{2\varphi H_f (m_{a1}+2\,m_{a2})}(m_{a1}-m_{a2})(m_{a2}+m_{a3}) - e^{2\,H_f (m_{a2}+\varphi m_{a3})}(-m_{a1}+m_{a2})(m_{a2}+m_{a3}) - e^{4\varphi H_f m_{a2}}(m_{a1}+m_{a2})(m_{a2}+m_{a3}) + e^{2\,H_f (m_{a2}+\varphi(m_{a1}+m_{a3}))}(m_{a1}+m_{a2})(m_{a2}+m_{a3}))\right)\right)$$

$$B_{2,5} = \left(-\left(2\,e^{\varphi H_f m_{a3}}\left(e^{H_f m_{a2}} - e^{\varphi H_f m_{a2}}\right)\left(e^{H_f m_{a2}}(m_{a1}-m_{a2}) + e^{2\varphi H_f (m_{a1}+m_{a2})}(-m_{a1}+m_{a2}) - e^{2\varphi H_f m_{a2}}(m_{a1}+m_{a2}) + e^{H_f (2\varphi m_{a1}+m_{a2})}(m_{a1}+m_{a2})\right)m_{a3}\right)\Big/\left((-1+2\varphi)\,H_f m_{a2}\left(e^{2\varphi H_f (m_{a1}+2\,m_{a2}+m_{a3})}(m_{a1}-m_{a2})(m_{a2}-m_{a3}) + e^{2\,H_f m_{a2}}(-m_{a1}+m_{a2})(m_{a2}-m_{a3}) - e^{2\,H_f (\varphi m_{a1}+m_{a2})}(m_{a1}+m_{a2})(m_{a2} - m_{a3}) + e^{2\varphi H_f (2\,m_{a2}+m_{a3})}(m_{a1}+m_{a2})(m_{a2}-m_{a3}) - e^{2\varphi H_f (m_{a1}+2\,m_{a2})}(m_{a1}-m_{a2})(m_{a2}+m_{a3}) - e^{2\,H_f (m_{a2}+\varphi m_{a3})}(-m_{a1}+m_{a2})(m_{a2} + m_{a3}) - e^{4\varphi H_f m_{a2}}(m_{a1}+m_{a2})(m_{a2}+m_{a3}) + e^{2\,H_f (m_{a2}+\varphi(m_{a1}+m_{a3}))}(m_{a1}+m_{a2})(m_{a2}+m_{a3}))\right)\right)$$

A.3. Components of $B_{3,j}$

$$B_{3,1} = \Big(2\,e^{(1+2\varphi)H_f m_{a2}}\big(-1+e^{\varphi H_f m_{a1}}\big)^2\big(-1+e^{\varphi H_f m_{a3}}\big)^2 m_{a1}m_{a2}\Big)\Big/\big(\varphi H_f m_{a3}\big(e^{2\varphi H_f (m_{a1}+2\,m_{a2}+m_{a3})}(m_{a1}-m_{a2})(m_{a2}-m_{a3}) + e^{2\,H_f m_{a2}}(-m_{a1}+m_{a2})$$
$$\times(m_{a2}-m_{a3}) - e^{2\,H_f(\varphi m_{a1}+m_{a2})}(m_{a1}+m_{a2})(m_{a2}-m_{a3}) + e^{2\varphi H_f(2\,m_{a2}+m_{a3})}(m_{a1}+m_{a2})(m_{a2}-m_{a3}) - e^{2\varphi H_f(m_{a1}+2\,m_{a2})}(m_{a1}-m_{a2})(m_{a2}$$
$$+m_{a3}) - e^{2\,H_f(m_{a2}+\varphi m_{a3})}(-m_{a1}+m_{a2})(m_{a2}+m_{a3}) - e^{4\varphi H_f m_{a2}}(m_{a1}+m_{a2})(m_{a2}+m_{a3}) + e^{2\,H_f(m_{a2}+\varphi(m_{a1}+m_{a3}))}(m_{a1}+m_{a2})(m_{a2}+m_{a3})\big)\big)$$

$$B_{3,2} = \Big(\Big(\big(e^{H_f m_{a2}} - e^{2\varphi H_f m_{a2}}\big)\big(-1+e^{\varphi H_f m_{a3}}\big)^2 m_{a2}\big(e^{H_f m_{a2}}(m_{a1}-m_{a2}) + e^{2\varphi H_f(m_{a1}+m_{a2})}(-m_{a1}+m_{a2}) - e^{2\varphi H_f m_{a2}}(m_{a1}+m_{a2}) + e^{H_f(2\varphi m_{a1}+m_{a2})}(m_{a1}$$
$$+m_{a2})\big)\Big)\Big/\big(\varphi H_f m_{a3}\big(e^{2\varphi H_f(m_{a1}+2\,m_{a2}+m_{a3})}(m_{a1}-m_{a2})(m_{a2}-m_{a3}) + e^{2\,H_f m_{a2}}(-m_{a1}+m_{a2})(m_{a2}-m_{a3}) - e^{2\,H_f(\varphi m_{a1}+m_{a2})}(m_{a1}+m_{a2})(m_{a2}$$
$$-m_{a3}) + e^{2\varphi H_f(2\,m_{a2}+m_{a3})}(m_{a1}+m_{a2})(m_{a2}-m_{a3}) - e^{2\varphi H_f(m_{a1}+2\,m_{a2})}(m_{a1}-m_{a2})(m_{a2}+m_{a3}) - e^{2\,H_f(m_{a2}+\varphi m_{a3})}(-m_{a1}+m_{a2})(m_{a2}+m_{a3})$$
$$-e^{4\varphi H_f m_{a2}}(m_{a1}+m_{a2})(m_{a2}+m_{a3}) + e^{2\,H_f(m_{a2}+\varphi(m_{a1}+m_{a3}))}(m_{a1}+m_{a2})(m_{a2}+m_{a3})\big)\big)\Big)$$

$$\big(B_{3,3} = \big(-\big(\big(-1+e^{\varphi H_f m_{a3}}\big)\big(e^{\varphi H_f(2\,m_{a1}+4\,m_{a2}+m_{a3})}(m_{a1}-m_{a2})(2\,m_{a2}-m_{a3}) + e^{2\,H_f m_{a2}}(-m_{a1}+m_{a2})(2m_{a2}-m_{a3}) - e^{2\,H_f(\varphi m_{a1}+m_{a2})}(m_{a1}+m_{a2})$$
$$\times(2\,m_{a2}-m_{a3}) + e^{\varphi H_f(4\,m_{a2}+m_{a3})}(m_{a1}+m_{a2})(2\,m_{a2}-m_{a3}) - e^{2\varphi H_f(m_{a1}+2\,m_{a2})}(m_{a1}-m_{a2})(2\,m_{a2}+m_{a3}) - e^{2\,H_f m_{a2}+\varphi H_f m_{a3}}(-m_{a1}+m_{a2})$$
$$\times(2\,m_{a2}+m_{a3}) - e^{4\varphi H_f m_{a2}}(m_{a1}+m_{a2})(2m_{a2}+m_{a3}) + e^{H_f(2\,m_{a2}+\varphi(2\,m_{a1}+m_{a3}))}(m_{a1}+m_{a2})(2\,m_{a2}+m_{a3})\big)\big)$$
$$/\big(\varphi H_f m_{a3}\big(e^{2\varphi H_f(m_{a1}+2\,m_{a2}+m_{a3})}(m_{a1}-m_{a2})(m_{a2}-m_{a3}) + e^{2\,H_f m_{a2}}(-m_{a1}+m_{a2})\,(m_{a2}-m_{a3}) - e^{2\,H_f(\varphi m_{a1}+m_{a2})}(m_{a1}+m_{a2})(m_{a2}-m_{a3})$$
$$+e^{2\varphi H_f(2\,m_{a2}+m_{a3})}(m_{a1}+m_{a2})(m_{a2}-m_{a3}) - e^{2\varphi H_f(m_{a1}+2\,m_{a2})}(m_{a1}-m_{a2})(m_{a2}+m_{a3}) - e^{2\,H_f(m_{a2}+\varphi m_{a3})}(-m_{a1}+m_{a2})(m_{a2}+m_{a3})$$
$$-e^{4\varphi H_f m_{a2}}(m_{a1}+m_{a2})(m_{a2}+m_{a3}) + e^{2\,H_f(m_{a2}+\varphi(m_{a1}+m_{a3}))}(m_{a1}+m_{a2})(m_{a2}+m_{a3})\big)\big)\big)\big)$$

$$B_{3,4} = \Big(-\Big(4\,e^{H_f(m_{a2}+\varphi(m_{a1}+2\,m_{a2}))}\big(-1+e^{\varphi H_f m_{a3}}\big)^2 m_{a1}m_{a2}\Big)\Big)\Big/\big(\varphi H_f m_{a3}\big(-e^{2\varphi H_f(m_{a1}+2\,m_{a2}+m_{a3})}(m_{a1}-m_{a2})(m_{a2}-m_{a3}) - e^{2\,H_f m_{a2}}(-m_{a1}+m_{a2})$$
$$\times(m_{a2}-m_{a3}) + e^{2\,H_f(\varphi m_{a1}+m_{a2})}(m_{a1}+m_{a2})(m_{a2}-m_{a3}) - e^{2\varphi H_f(2\,m_{a2}+m_{a3})}(m_{a1}+m_{a2})(m_{a2}-m_{a3}) + e^{2\varphi H_f(m_{a1}+2\,m_{a2})}(m_{a1}-m_{a2})(m_{a2}$$
$$+m_{a3}) + e^{2\,H_f(m_{a2}+\varphi m_{a3})}(-m_{a1}+m_{a2})(m_{a2}+m_{a3}) + e^{4\varphi H_f m_{a2}}(m_{a1}+m_{a2})(m_{a2}+m_{a3}) - e^{2\,H_f(m_{a2}+\varphi(m_{a1}+m_{a3}))}(m_{a1}+m_{a2})(m_{a2}+m_{a3})\big)\big)$$

$$B_{3,5} = \big(\big(\big(-1+e^{\varphi H_f m_{a3}}\big)\big(e^{\varphi H_f(2\,m_{a1}+4\,m_{a2}+m_{a3})}(m_{a1}-m_{a2})(m_{a2}-m_{a3}) + e^{2\,H_f m_{a2}}(-m_{a1}+m_{a2})(m_{a2}-m_{a3}) - e^{2\,H_f(\varphi m_{a1}+m_{a2})}(m_{a1}+m_{a2})(m_{a2}$$
$$-m_{a3}) + e^{\varphi H_f(4\,m_{a2}+m_{a3})}(m_{a1}+m_{a2})(m_{a2}-m_{a3}) - e^{2\varphi H_f(m_{a1}+2\,m_{a2})}(m_{a1}-m_{a2})(m_{a2}+m_{a3}) - e^{2\,H_f m_{a2}+\varphi H_f m_{a3}}(-m_{a1}+m_{a2})(m_{a2}+m_{a3})$$
$$-e^{4\varphi H_f m_{a2}}(m_{a1}+m_{a2})(m_{a2}+m_{a3}) + e^{H_f(2\,m_{a2}+\varphi(2\,m_{a1}+m_{a3}))}(m_{a1}+m_{a2})(m_{a2}+m_{a3})\big)\big)\big/\big(\varphi H_f m_{a3}\big(e^{2\varphi H_f(m_{a1}+2\,m_{a2}+m_{a3})}(m_{a1}-m_{a2})(m_{a2}-m_{a3})$$
$$+e^{2\,H_f m_{a2}}(-m_{a1}+m_{a2})(m_{a2}-m_{a3}) - e^{2\,H_f(\varphi m_{a1}+m_{a2})}(m_{a1}+m_{a2})(m_{a2}-m_{a3}) + e^{2\varphi H_f(2\,m_{a2}+m_{a3})}(m_{a1}+m_{a2})(m_{a2}-m_{a3})$$
$$-e^{2\varphi H_f(m_{a1}+2\,m_{a2})}(m_{a1}-m_{a2})(m_{a2}+m_{a3}) - e^{2\,H_f(m_{a2}+\varphi m_{a3})}(-m_{a1}+m_{a2})(m_{a2}+m_{a3}) - e^{4\varphi H_f m_{a2}}(m_{a1}+m_{a2})(m_{a2}+m_{a3})$$
$$+e^{2\,H_f(m_{a2}+\varphi(m_{a1}+m_{a3}))}(m_{a1}+m_{a2})(m_{a2}+m_{a3})\big)\big)\big)$$

A.4. Components of $C_{1,j}$

$$C_{1,1} = \big(\big(-1+e^{\varphi H_f\ m_{a1}}\big)m_{a1}\big(e^{\varphi H_f(m_{a1}+4\,m_{a2}+2\,m_{a3})}(m_{a1}-m_{a2})(m_{a2}-m_{a3}) + e^{2\,H_f\ m_{a2}}(-m_{a1}+m_{a2})(m_{a2}-m_{a3}) - e^{\varphi H_f\ m_{a1}+2\,H_f\ m_{a2}}(m_{a1}+m_{a2})$$
$$\times(m_{a2}-m_{a3}) + e^{2\varphi H_f(2m_{a2}+m_{a3})}(m_{a1}+m_{a2})(m_{a2}-m_{a3}) - e^{\varphi H_f(m_{a1}+4\,m_{a2})}(m_{a1}-m_{a2})(m_{a2}+m_{a3}) - e^{2\,H_f(m_{a2}+\varphi m_{a3})}(-m_{a1}+m_{a2})(m_{a2}$$
$$+m_{a3}) - e^{4\varphi H_f m_{a2}}(m_{a1}+m_{a2})(m_{a2}+m_{a3}) + e^{H_f(2\,m_{a2}+\varphi(m_{a1}+2\,m_{a3}))}(m_{a1}+m_{a2})\,(m_{a2}+m_{a3})\big)\big)\big/\big(e^{2\varphi H_f(m_{a1}+2\,m_{a2}+m_{a3})}(m_{a1}-m_{a2})(m_{a2}-m_{a3})$$
$$+e^{2H_f m_{a2}}(-m_{a1}+m_{a2})(m_{a2}-m_{a3}) - e^{2\,H_f(\varphi m_{a1}+m_{a2})}(m_{a1}+m_{a2})(m_{a2}-m_{a3}) + e^{2\varphi H_f(2\,m_{a2}+m_{a3})}(m_{a1}+m_{a2})(m_{a2}-m_{a3})$$
$$-e^{2\varphi H_f(m_{a1}+2\,m_{a2})}(m_{a1}-m_{a2})(m_{a2}+m_{a3}) - e^{2H_f(m_{a2}+\varphi m_{a3})}(-m_{a1}+m_{a2})(m_{a2}+m_{a3}) - e^{4\varphi H_f m_{a2}}(m_{a1}+m_{a2})(m_{a2}+m_{a3})$$
$$+e^{2\,H_f(m_{a2}+\varphi(m_{a1}+m_{a3}))}(m_{a1}+m_{a2})(m_{a2}+m_{a3})\big)$$

$$C_{1,2} = \big(\big(2e^{\varphi H_f m_{a1}}\big(e^{H_f m_{a2}} - e^{2\varphi H_f m_{a2}}\big)m_{a1}m_{a2}\big(e^{2\varphi H_f(m_{a2}+m_{a3})}(m_{a2}-m_{a3}) + e^{H_f m_{a2}}(-m_{a2}+m_{a3}) - e^{2\varphi H_f m_{a2}}\big)(m_{a2}+m_{a3}) + e^{H_f(m_{a2}+2\varphi m_{a3})}(m_{a2}+m_{a3})$$
$$\times(m_{a1}-m_{a2})(m_{a2}+m_{a3}) - e^{2\,H_f(m_{a2}+\varphi m_{a3})}(-m_{a1}+m_{a2})(m_{a2}+m_{a3}) - e^{4\varphi H_f m_{a2}}(m_{a1}+m_{a2})\big)\big)\big/\big(e^{2\varphi H_f(m_{a1}+2\,m_{a2}+m_{a3})}(m_{a1}-m_{a2})\,(m_{a2}$$
$$-m_{a3}) + e^{2\,H_f m_{a2}}(-m_{a1}+m_{a2})(m_{a2}-m_{a3}) - e^{2\,H_f(\varphi m_{a1}+m_{a2})}(m_{a1}+m_{a2})(m_{a2}-m_{a3}) + e^{2\varphi H_f(2\,m_{a2}+m_{a3})}(m_{a1}+m_{a2})(m_{a2}-m_{a3})$$
$$-e^{2\varphi H_f(m_{a1}+2\,m_{a2})}(m_{a2}+m_{a3}) + e^{2\,H_f(m_{a2}+\varphi(m_{a1}+m_{a3}))}(m_{a1}+m_{a2})(m_{a2}+m_{a3})\big)$$

$$C_{1,3} = \Big(\Big(4e^{H_f(m_{a2}+\varphi(m_{a1}+2\ m_{a2}))}\big(-1+e^{\varphi H_f m_{a3}}\big)^2 m_{a1}m_{a2}m_{a3}\Big)\Big/\big(e^{2\varphi H_f(m_{a1}+2\ m_{a2}+m_{a3})}(m_{a1}-m_{a2})(m_{a2}-m_{a3})+e^{2\ H_f m_{a2}}(-m_{a1}+m_{a2})(m_{a2}-m_{a3})$$
$$-e^{2\ H_f(\varphi m_{a1}+m_{a2})}(m_{a1}+m_{a2})(m_{a2}-m_{a3})+e^{2\varphi H_f(2\ m_{a2}+m_{a3})}(m_{a1}+m_{a2})(m_{a2}-m_{a3})-e^{2\varphi H_f(m_{a1}+2\ m_{a2})}(m_{a1}-m_{a2})(m_{a2}+m_{a3})$$
$$-e^{2\ H_f(m_{a2}+\varphi m_{a3})}(-m_{a1}+m_{a2})(m_{a2}+m_{a3})-e^{4\varphi H_f m_{a2}}(m_{a1}+m_{a2})(m_{a2}+m_{a3})+e^{2\ H_f(m_{a2}+\varphi(m_{a1}+m_{a3}))}(m_{a1}+m_{a2})(m_{a2}+m_{a3})\big)\Big)$$

$$C_{1,4} = \big(-\big(m_{a1}\big(e^{2\varphi H_f(m_{a1}+2\ m_{a2}+m_{a3})}(m_{a1}-m_{a2})(m_{a2}-m_{a3})-e^{2\ H_f m_{a2}}(-m_{a1}+m_{a2})(m_{a2}-m_{a3})-e^{2\ H_f(\varphi m_{a1}+m_{a2})}(m_{a1}+m_{a2})(m_{a2}-m_{a3})$$
$$-e^{2\varphi H_f(2\ m_{a2}+m_{a3})}(m_{a1}+m_{a2})(m_{a2}-m_{a3})-e^{2\varphi H_f(m_{a1}+2\ m_{a2})}(m_{a1}-m_{a2})(m_{a2}+m_{a3})+e^{2\ H_f(m_{a2}+\varphi m_{a3})}(-m_{a1}+m_{a2})(m_{a2}+m_{a3})$$
$$+e^{4\varphi H_f m_{a2}}(m_{a1}+m_{a2})(m_{a2}+m_{a3})+e^{2\ H_f(m_{a2}+\varphi(m_{a1}+m_{a3}))}(m_{a1}+m_{a2})(m_{a2}+m_{a3})\big)\big)\big/\big(e^{2\varphi H_f(m_{a1}+2\ m_{a2}+m_{a3})}(m_{a1}-m_{a2})(m_{a2}-m_{a3})$$
$$+e^{2\ H_f m_{a2}}(-m_{a1}+m_{a2})(m_{a2}-m_{a3})-e^{2\ H_f(\varphi m_{a1}+m_{a2})}(m_{a1}+m_{a2})(m_{a2}-m_{a3})+e^{2\varphi H_f(2\ m_{a2}+m_{a3})}(m_{a1}+m_{a2})(m_{a2}-m_{a3})$$
$$-e^{2\varphi H_f(m_{a1}+2\ m_{a2})}(m_{a1}-m_{a2})(m_{a2}+m_{a3})-e^{2\ H_f(m_{a2}+\varphi m_{a3})}(-m_{a1}+m_{a2})(m_{a2}+m_{a3})-e^{4\varphi H_f m_{a2}}(m_{a1}+m_{a2})(m_{a2}+m_{a3})$$
$$+e^{2\ H_f(m_{a2}+\varphi(m_{a1}+m_{a3}))}(m_{a1}+m_{a2})(m_{a2}+m_{a3})\big)\big)$$

$$C_{1,5} = \big(\big(8e^{H_f(m_{a2}+\varphi(m_{a1}+2\ m_{a2}+m_{a3}))}m_{a1}m_{a2}m_{a3}\big)\big/\big(e^{4\varphi H_f m_{a2}}(m_{a1}+m_{a2})\big(-m_{a2}+e^{2\varphi H_f m_{a3}}(m_{a2}-m_{a3})-m_{a3}\big)+e^{2\ H_f m_{a2}}(m_{a1}-m_{a2})\big(-m_{a2}+m_{a3}$$
$$+e^{2\varphi H_f m_{a3}}(m_{a2}+m_{a3})\big)+e^{2\varphi H_f m_{a1}}\big(e^{4\varphi H_f m_{a2}}(m_{a1}-m_{a2})\big(-m_{a2}+e^{2\varphi H_f m_{a3}}(m_{a2}-m_{a3})-m_{a3}\big)+e^{2\ H_f m_{a2}}(m_{a1}+m_{a2})\big(-m_{a2}+m_{a3}$$
$$+e^{2\varphi H_f m_{a3}}(m_{a2}+m_{a3})\big)\big)\big)\big)$$

A.5. *Components of* $C_{2,j}$

$$C_{2,1} = -\Big(4\,e^{H_f(m_{a2}+2\varphi m_{a2}+\varphi m_{a3})}\big(-1+e^{\varphi H_f m_{a1}}\big)^2 m_{a1}m_{a2}m_{a3}\Big)\Big/\big(e^{2\varphi H_f(m_{a1}+2\ m_{a2}+m_{a3})}(m_{a1}-m_{a2})(m_{a2}-m_{a3})+e^{2\ H_f m_{a2}}(-m_{a1}+m_{a2})(m_{a2}-m_{a3})$$
$$-e^{2\ H_f(\varphi m_{a1}+m_{a2})}(m_{a1}+m_{a2})(m_{a2}-m_{a3})+e^{2\varphi H_f(2\ m_{a2}+m_{a3})}(m_{a1}+m_{a2})(m_{a2}-m_{a3})-e^{2\varphi H_f(m_{a1}+2\ m_{a2})}(m_{a1}-m_{a2})(m_{a2}+m_{a3})$$
$$-e^{2\ H_f(m_{a2}+\varphi m_{a3})}(-m_{a1}+m_{a2})(m_{a2}+m_{a3})-e^{4\varphi H_f m_{a2}}(m_{a1}+m_{a2})(m_{a2}+m_{a3})+e^{2\ H_f(m_{a2}+\varphi(m_{a1}+m_{a3}))}(m_{a1}+m_{a2})(m_{a2}+m_{a3})\big)$$

$$C_{2,2} = \big(-\big(2e^{\varphi H_f m_{a3}}\big(e^{H_f m_{a2}}-e^{2\varphi H_f m_{a2}}\big)m_{a2}\big(e^{H_f m_{a2}}(m_{a1}-m_{a2})+e^{2\varphi H_f(m_{a1}+m_{a2})}(-m_{a1}+m_{a2})-e^{2\varphi H_f m_{a2}}(m_{a1}+m_{a2})+e^{H_f(2\varphi m_{a1}+m_{a2})}(m_{a1}+m_{a2})\big)m_{a3}\big)$$
$$\big/\big(e^{2\varphi H_f(m_{a1}+2\,m_{a2}+m_{a3})}(m_{a1}-m_{a2})(m_{a2}-m_{a3})+e^{2\,H_f m_{a2}}(-m_{a1}+m_{a2})(m_{a2}-m_{a3})-e^{2\,H_f(\varphi m_{a1}+m_{a2})}(m_{a1}+m_{a2})(m_{a2}-m_{a3})+e^{2\varphi H_f(2\,m_{a2}+m_{a3})}(m_{a1}$$
$$+m_{a2})(m_{a2}-m_{a3})-e^{2\varphi H_f(m_{a1}+2\,m_{a2})}(m_{a1}-m_{a2})(m_{a2}+m_{a3})-e^{2\,H_f(m_{a2}+\varphi m_{a3})}(-m_{a1}+m_{a2})(m_{a2}+m_{a3})-e^{4\varphi H_f m_{a2}}(m_{a1}+m_{a2})(m_{a2}+m_{a3})$$
$$+e^{2\,H_f(m_{a2}+\varphi(m_{a1}+m_{a3}))}(m_{a1}+m_{a2})(m_{a2}+m_{a3})\big)\big)$$

$$C_{2,3} = \big(-\big(\big(-1+e^{\varphi H_f m_{a3}}\big)m_{a3}\big)\big(e^{\varphi H_f(2\ m_{a1}+4\ m_{a2}+m_{a3})}(m_{a1}-m_{a2})(m_{a2}-m_{a3})+e^{2\ H_f m_{a2}}(-m_{a1}+m_{a2})(m_{a2}-m_{a3})-e^{2\ H_f(\varphi m_{a1}+m_{a2})}(m_{a1}+m_{a2})$$
$$\times(m_{a2}-m_{a3})+e^{\varphi H_f(4\ m_{a2}+m_{a3})}(m_{a1}+m_{a2})(m_{a2}-m_{a3})-e^{2\varphi H_f(m_{a1}+2\ m_{a2})}(m_{a1}-m_{a2})(m_{a2}+m_{a3})-e^{2\ H_f m_{a2}+\varphi H_f m_{a3}}(-m_{a1}+m_{a2})(m_{a2}$$
$$+m_{a3})-e^{4\varphi H_f m_{a2}}(m_{a1}+m_{a2})(m_{a2}+m_{a3})+e^{H_f(2\ m_{a2}+\varphi(2\ m_{a1}+m_{a3}))}(m_{a1}+m_{a2})(m_{a2}+m_{a3})\big)\big)\big/\big(e^{2\varphi H_f(m_{a1}+2\ m_{a2}+m_{a3})}(m_{a1}-m_{a2})(m_{a2}-m_{a3})$$
$$+e^{2\ H_f m_{a2}}(-m_{a1}+m_{a2})(m_{a2}-m_{a3})-e^{2\ H_f(\varphi m_{a1}+m_{a2})}(m_{a1}+m_{a2})(m_{a2}-m_{a3})+e^{2\varphi H_f(2\ m_{a2}+m_{a3})}(m_{a1}+m_{a2})(m_{a2}-m_{a3})$$
$$-e^{2\varphi H_f(m_{a1}+2\ m_{a2})}(m_{a1}-m_{a2})(m_{a2}+m_{a3})-e^{2\ H_f(m_{a2}+\varphi m_{a3})}(-m_{a1}+m_{a2})(m_{a2}+m_{a3})-e^{4\varphi H_f m_{a2}}(m_{a1}+m_{a2})(m_{a2}+m_{a3})$$
$$+e^{2\ H_f(m_{a2}+\varphi(m_{a1}+m_{a3}))}(m_{a1}+m_{a2})(m_{a2}+m_{a3})\big)$$

$$C_{2,4} = \big(-\big(8\,e^{H_f(m_{a2}+\varphi(m_{a1}+2\ m_{a2}+m_{a3}))}m_{a1}m_{a2}m_{a3}\big)\big/\big(e^{2\varphi H_f(m_{a1}+2m_{a2}+m_{a3})}(m_{a1}-m_{a2})(m_{a2}-m_{a3})+e^{2H_f m_{a2}}(-m_{a1}+m_{a2})(m_{a2}-m_{a3})$$
$$-e^{2H_f(\varphi m_{a1}+m_{a2})}(m_{a1}+m_{a2})(m_{a2}-m_{a3})+e^{2\varphi H_f(2\ m_{a2}+m_{a3})}(m_{a1}+m_{a2})(m_{a2}-m_{a3})-e^{2\varphi H_f(m_{a1}+2m_{a2})}(m_{a1}-m_{a2})(m_{a2}+m_{a3})$$
$$-e^{2H_f(m_{a2}+\varphi m_{a3})}(-m_{a1}+m_{a2})(m_{a2}+m_{a3})-e^{4\varphi H_f m_{a2}}(m_{a1}+m_{a2})(m_{a2}+m_{a3})+e^{2H_f(m_{a2}+\varphi(m_{a1}+m_{a3}))}(m_{a1}+m_{a2})(m_{a2}+m_{a3})\big)\big)$$

$$C_{2,5} = \big(\big(m_{a3}\big(e^{2\varphi H_f(m_{a1}+2\ m_{a2}+m_{a3})}(m_{a1}-m_{a2})(m_{a2}-m_{a3})-e^{2\ H_f m_{a2}}(-m_{a1}+m_{a2})(m_{a2}-m_{a3})+e^{2\ H_f(\varphi m_{a1}+m_{a2})}(m_{a1}+m_{a2})(m_{a2}-m_{a3})$$
$$+e^{2\varphi H_f(2m_{a2}+m_{a3})}(m_{a1}+m_{a2})(m_{a2}-m_{a3})+e^{2\varphi H_f(m_{a1}+2m_{a2})}(m_{a1}-m_{a2})(m_{a2}+m_{a3})-e^{2\ H_f(m_{a2}+\varphi m_{a3})}(-m_{a1}+m_{a2})(m_{a2}+m_{a3})$$
$$+e^{4\varphi H_f m_{a2}}(m_{a1}+m_{a2})(m_{a2}+m_{a3})+e^{2\ H_f(m_{a2}+\varphi(m_{a1}+m_{a3}))}(m_{a1}+m_{a2})(m_{a2}+m_{a3})\big)\big)\big/\big(e^{2\varphi H_f(m_{a1}+2\ m_{a2}+m_{a3})}(m_{a1}-m_{a2})(m_{a2}-m_{a3})$$
$$+e^{2\ H_f m_{a2}}(-m_{a1}+m_{a2})(m_{a2}-m_{a3})-e^{2\ H_f(\varphi m_{a1}+m_{a2})}(m_{a1}+m_{a2})(m_{a2}-m_{a3})+e^{2\varphi H_f(2\ m_{a2}+m_{a3})}(m_{a1}+m_{a2})(m_{a2}-m_{a3})$$
$$-e^{2\varphi H_f(m_{a1}+2\ m_{a2})}(m_{a1}-m_{a2})(m_{a2}+m_{a3})-e^{2\ H_f(m_{a2}+\varphi m_{a3})}(-m_{a1}+m_{a2})(m_{a2}+m_{a3})-e^{4\varphi H_f m_{a2}}(m_{a1}+m_{a2})(m_{a2}+m_{a3})$$
$$+e^{2\ H_f(m_{a2}+\varphi(m_{a1}+m_{a3}))}(m_{a1}+m_{a2})(m_{a2}+m_{a3})\big)\big)$$

REFERENCES

Asinari, P., Cecchinato, L., Fornasieri, E., 2004. Effects of thermal conduction in microchannel gas coolers for carbon dioxide. Int. J. Refrigeration 27 (6), 577–586.

Asinari, P., 2004. Finite-volume and finite-element hybrid technique for the calculation of complex heat exchangers by Semiexplicit method for wall temperature linked equations (SEWTLE). Numer. Heat Transfer Part B-Fundamentals 45, 221–247.

Cavallini, A., Censi, G., Del Col, D., Doretti, L., Longo, G.A., Rossetto, L., 2002. In-tube condensation of halogenated refrigerants. ASHRAE Trans. 108 (1), 146–161.

Chisholm, D., 1972. An Equation for Velocity Ratio in Two-Phase Flow. NEL Report 535.

Churchill, S.W., 1977. Friction-factor equation spans all fluid flow regimes. Chem. Eng. 7, 91–92.

CoilDesigner, 2010. Tool to Aid in the Design, Simulation and Optimization of Air-Cooled Heat Exchangers. University of Maryland, Center for Environmental Energy Engineering, MD, USA. http://ceee.umd.edu/isoc/software/index_coildesigner.htm.

Corberán, J.M., Gonzálvez, J., Montes, P., Blasco, R., 2002. 'ART' a computer code to assist the design of refrigeration and A/C equipment. In: International Refrigeration and Air Conditioning Conference at Purdue, IN, USA.

Corberán, J.M., De Cordoba, P.F., Gonzalvez, J., Alias, F., 2001. Semiexplicit method for wall temperature linked equations (SEWTLE): a general finite-volume technique for the calculation of complex heat exchangers. Numer. Heat Transfer, Part B 40, 37–59.

EVAP-COND, 2010. Simulation Models for Finned Tube Heat Exchangers with Circuitry Optimization. National Institute of Standards and Technology, Building and Fire Research Laboratory, Gaithersburg, MD, USA. http://www.nist.gov/el/building_environment/evapcond_software.cfm.

Friedel, L., 1980. Pressure drop during gas/vapor-liquid flow in pipes. Int. Chem. Eng. 20, 352–367.

Fronk, B.M., Garimella, S., 2011. Water-coupled carbon dioxide microchannel gas cooler for heat pump water heaters: Part II– Model development and validation. Int. J. Refrigeration 34, 17–28.

García-Cascales, J.R., Vera-García, F., Gonzálvez-Maciá, J., Corberán-Salvador, J.M., Johnson, M.W., Kohler, G.T., 2010. Compact heat exchangers modeling: condensation. Int. J. Refrigeration 33, 135–147.

Gnielinski, V., 1976. New equations for heat and mass transfer in turbulent pipe and channel flow. Int. Chem. Eng. 16 (2), 359–368.

IMST-ART, 2010. Simulation Tool to Assist the Selection, Design and Optimization of Refrigeration Equipment and Components. Universitat Politècnica de Valéncia, Instituto de IngenieríaEnergética, Spain. http://www.imst-art.com.

Incropera, F.P., DeWitt, D.P., 1996. Fundamentals of Heat and Mass Transfer, fourth ed. John Wiley and Sons, New York.

Jiang, H.B., Aute, V., Radermacher, R., 2006. Coildesigner: a general-purpose simulation and design tool for air-to-refrigerant heat exchangers. Int. J. Refrigeration 29 (4), 601–610.

Kays, W.M., London, A.L., 1984. Compact Heat Exchangers, third ed. McGraw-Hill, New York.

Kim, M.-H., Bullard, C., 2002. Air-side thermal hydraulic performance of multi-louvered fin Aluminum heat exchangers. Int. J. Refrigeration 25, 390–400.

Lee, J., Domanski, P.A., July 1997. Impact of Air and Refrigerant Maldistributions on the Performance of Finned-Tube Evaporators with R-22 and R-407C. Report No.: DOE/CE/23810-23881.

Martínez-Ballester, S., Corberán, J.M., Gonzálvez-Macia, J. Numerical model for microchannel condensers and gas coolers: Part II –Simulation studies and models comparison, Int. J. Refrigeration, Submitted for publication.

Martínez-Ballester, S., Corberán, J.M., Gonzálvez-Macia, J., Domanski, P.A., 2011. Impact of classical assumptions in modelling a microchannel gas cooler. Int. J. Refrigeration 34, 1898–1910.

Patankar, S.V., 1980. Numerical Heat Transfer and Fluid Flow. Hemisphere, New York.

Shao, L.L., Yang, L., Zhang, C.L., Gu, B., 2009. Numerical modeling of serpentine microchannel condensers. Int. J. Refrigeration 32 (6), 1162–1172.

Singh, V., Aute, V., Radermacher, R., 2008. Numerical approach for modeling air-to-refrigerant fin-and-tube heat exchanger with tube-to-tube heat transfer. Int. J. Refrigeration 31 (8), 1414–1425.

Yin, J.M., Bullard, C.W., Hrnjak, P.S., 2001. R-744 gas cooler model development and validation. Int. J. Refrigeration 24 (7), 692–701.

Yin, J.M., Bullard, C.W., Hrnjak, P.S., 2000. Pressure Drop Measurements in Microchannel Heat Exchanger. University of Illinois at Urbana-Champaign. CR-40.